AMERICAN SOCIETY FOR MICROBIOLOGY | Journal of Virology®

VIRUS-CELL INTERACTIONS

Cellular p32 Is a Critical Regulator of Porcine Circovirus Type 2 Nuclear Egress

Tongtong Wang,[a,f] Qian Du,[a] Yingying Niu,[a] Xiaohua Zhang,[a] Zhenyu Wang,[a] Xingchen Wu,[a] XueFeng Yang,[a] Xiaomin Zhao,[a] Shan-Lu Liu,[b,c,d,e] Dewen Tong,[a] Yong Huang[a]

[a]College of Veterinary Medicine, Northwest A&F University, Yangling, China
[b]Center for Retrovirus Research, The Ohio State University, Columbus, Ohio, USA
[c]Viruses and Emerging Pathogens Program, Infectious Diseases Institute, The Ohio State University, Columbus, Ohio, USA
[d]Department of Veterinary Biosciences, The Ohio State University, Columbus, Ohio, USA
[e]Department of Microbial Infection and Immunity, The Ohio State University, Columbus, Ohio, USA
[f]College of Agronomy, Liaocheng University, Liaocheng, China

ABSTRACT Circoviruses are the smallest DNA viruses known to infect mammalian and avian species. Although circoviruses are known to be associated with a range of clinical diseases, the details of circovirus DNA release still remain unknown. Here, we identified p32 as a key regulator for porcine circoviral nuclear egress. Upon porcine circovirus type 2 (PCV2) infection, p32 was recruited into the nucleus by the viral capsid (Cap) protein; simultaneously, protein kinase C isoform δ (PKC-δ) was phosphorylated at threonine 505 by phospholipase C (PLC)-mediated signaling at the early stage of infection, which was further amplified by Jun N-terminal protein kinase (JNK) and extracellular signal-regulated kinase (ERK) signaling at the late infection phase. p32 functioned as an adaptor to recruit phosphorylated PKC-δ and Cap to the nuclear membrane to phosphorylate lamin A/C, resulting in a rearrangement of nuclear lamina and thus facilitating viral nuclear egress. Consistent with these findings, knockout (KO) of p32 in PCV2-infected cells markedly reduced the phosphorylation of PKC-δ and impeded the recruitment of p-PKC-δ and Cap to the nuclear membrane, hence abolishing the phosphorylation of lamin A/C and the rearrangement of nuclear lamina. As a result, p32 depletion profoundly impaired the production of cell-free viruses during PCV2 infection. We further identified the N-terminal 24RRR26 of Cap to be crucial for binding to p32, and mutation of these three arginine residues significantly weakened the replication and pathogenesis of PCV2 *in vivo*. In summary, our findings highlight a critical role of p32 in the activation and recruitment of PKC-δ to phosphorylate lamin A/C and facilitate porcine circoviral nuclear egress, and they certainly help understanding of the mechanism of PCV2 replication.

IMPORTANCE Circovirus infections are highly prevalent in mammalian and avian species. Circoviral capsid protein is the only structural protein of the virion that plays an essential role in viral assembly. However, the machinery of circovirus nuclear egress is currently unknown. In this work, we identified p32 as a key regulator of porcine circovirus type 2 (PCV2) nuclear egress that forms a complex with the viral capsid (Cap) protein to enhance protein kinase C isoform δ (PKC-δ) activity; this resulted in a recruitment of phosphorylated PKC-δ to the nuclear membrane, which further phosphorylates lamin A/C to promote the rearrangement of nuclear lamina and facilitate viral nuclear egress. Notably, we found that the N-terminal 24RRR26 of Cap, a highly conserved motif among circovirus species, was required for interacting with p32, and that mutation of this motif markedly impeded PCV2 nuclear egress. These data indicate that p32 is a critical regulator of PCV2 nuclear egress and reveal the importance of this finding in circovirus replication.

Citation Wang T, Du Q, Niu Y, Zhang X, Wang Z, Wu X, Yang X, Zhao X, Liu S-L, Tong D, Huang Y. 2019. Cellular p32 is a critical regulator of porcine circovirus type 2 nuclear egress. J Virol 93:e00979-19. https://doi.org/10.1128/JVI.00979-19.

Editor Rozanne M. Sandri-Goldin, University of California, Irvine

Address correspondence to Dewen Tong, dwtong@nwsuaf.edu.cn, or Yong Huang, yonghuang@nwsuaf.edu.cn.

T.W. and Q.D. contributed equally to this work.

Received 18 June 2019
Accepted 3 September 2019
Accepted manuscript posted online 11 September 2019
Published 13 November 2019

KEYWORDS PCV2, p32, regulator

Viruses are intracellular pathogens that are entirely dependent on the host machinery for replication (1). DNA viruses generally replicate their genomic DNA in the nucleus of infected cells and assemble and package their genomes into capsids within the nucleus; however, the formation of the mature virion takes place in the cell cytoplasm, requiring diverse strategies to deliver genome-containing capsid across the double-membrane nuclear envelope (NE) (2, 3). Many DNA viruses have evolved effective mechanisms to shuttle nucleocapsids from the nucleus to the cytoplasm, including destruction of NE continuity, alteration of the permeability of nuclear pores, and the membrane-budding pathway (envelopment/deenvelopment pathway) (2, 4–7). Viruses in the *Herpesviridae* family, which are large, enveloped, double-stranded DNA (dsDNA) viruses, because of the large size of their nucleocapsids (diameter, ~25 nm) that makes them unable to pass across the nuclear pore (5), usually do not depend on alteration of nuclear pores and disruption of nuclear membrane for their nuclear egress. Instead, herpesviruses dissolve the nuclear lamina, a dense meshwork under their inner nuclear membrane (INM), and then nucleocapsids bud from the nucleus into the INM and form enveloped particles in the perinuclear space; these perinuclear enveloped particles then fuse with the outer nuclear membranes (ONM), become deenveloped particles, and eventually are released to the cytoplasm (4, 8). Similarly, for viruses in the *Baculoviridae* family with circular dsDNA genomes packaged into rod-shaped, enveloped nucleocapsids (9, 10), the most common way of nuclear egress observed in studies of nucleopolyhedrovirus (NPV) is dependent on the membrane budding pathway (9, 11). Parvoviruses, which are nonenveloped single-stranded DNA viruses, traverse the NE via alteration of the permeability of nuclear pores or destruction of NE continuity (12). Circoviruses of the *Circoviridae* family are nonenveloped DNA viruses, and they can infect various domestic and wildlife animal species; so far, no studies have been carried out to address the nuclear egress strategies of this virus family.

The *Circoviridae* family contains two genera, *Gyrovirus* and *Circovirus* (13). The genus *Gyrovirus* has only one member, chicken anemia virus (CAV), which causes clinical disease and subclinical immunosuppression in chickens (13). In contrast, members of the genus *Circovirus* are pathogenic in various mammals, including pigs, dogs, minks, and palm civets, and they also have a broad host range in avian species, including geese, pigeons, canaries, and parrots, etc. (14–19). Porcine circovirus type 2 (PCV2), the most susceptible virus in pigs, is the major causative agent of porcine circovirus-associated diseases (PCVAD), which has a huge impact on swine production due to its immunosuppression function (20). Porcine circovirus type 3 (PCV3) has also recently been isolated from diseased pigs (21). Canine circovirus causes hemorrhagic enteritis in dogs (17), mink circovirus infection causes refractory diarrhea (19), beak and feather disease virus (BFDV) causes abnormal feathering and beak deformities in parrots and pigeons (14), and goose circovirus causes production losses and death in geese (22). Because of the increased morbidity of circovirus-associated diseases in both mammalian and avian hosts, as well as the emergence of cross-species transmission events of circoviruses in some species (23), circoviruses have attracted more and more attention.

Circoviruses contain a small circular, single-stranded ~2-kb DNA genome that has limited coding capacity; thus, the life cycle of circoviruses must depend on host factors and machineries (24). The capsid protein of circovirus has been identified as a pivotal regulator in the process of viral replication and the virus-host interaction (24). Thus, we hypothesized that the capsid protein, as well as its interacting cellular molecules, might carry out an important function in the nuclear egress of circoviruses. p32, also known as gC1qR, C1qBP, TAP, and HABP, is one of the interacting molecules of the PCV1 and PCV2 capsid (Cap) protein, and it has been reported to be an important mitochondrial matrix protein present on the cell surface and in the nucleus, as well as in the cytoplasm (25). p32 has been reported to be involved in the replication process of various viruses by binding to some specific viral proteins, such as herpes simplex virus 1 (HSV-1) UL47

and ICP34.5 (25, 26), human immunodeficiency virus Rev and Tat (27, 28), adenovirus core protein (29), hepatitis C virus core protein (30), Epstein-Barr virus (EBV) EBNA-1 (31), and human cytomegalovirus (HCMV) UL97, UL50, and UL53 proteins (32, 33). p32 is required for the phosphorylation and redistribution of nuclear lamina during the nuclear egress of HSV-1 via interaction with viral ICP34.5 (26) and has also been implicated in the nuclear egress of HCMV and EBV (33–35). Interestingly, p32 itself is not a kinase, and the only viral protein with kinase activity that has been shown to be associated with intracellular p32 is human CMV pUL97, which phosphorylates nuclear lamin at the inner nuclear membrane during the process of CMV infection (33). In cases where the interaction viral protein is not a kinase, viral infection can recruit and activate host kinase, such as protein kinase C isoform α (PKC-α) or protein kinase C isoform δ (PKC-δ), which phosphorylates nuclear lamin A/C, thus disrupting the nuclear lamina at the INM and allowing the capsid to bud into the perinuclear space (26). Although all PKC isoforms have been shown to interact with p32 *in vitro*, binding activities differ from one another depending on the activation state (36). For example, PKC-δ only binds with p32 in the presence of PKC activators; activated PKC-α and PKC-ζ show higher binding for p32, whereas other PKC isoforms (β, ε, θ, and μ) bind equally with p32 regardless of the presence of PKC activators (36). It is currently unclear how circovirus infection alters the nuclear membrane to release nucleocapsids into the cytoplasm; in particular, it is not known if and how p32 and PKC isotypes regulate the viral nuclear transport process.

In the present study, we used PCV2 as the infection model and investigated the role of p32 in circoviral nuclear egress. We found that, upon PCV2 infection, p32 was recruited into the nucleus by PCV2 Cap and functioned as an adaptor to transport nucleocapsids to the nuclear membrane; this led to a recruitment of p-PKC-δ to the nuclear membrane, which phosphorylated lamin A/C and thus promoted the rearrangement of nuclear lamin and facilitated PCV2 nuclear egress. We also found that knockout (KO) of p32, or mutation in the binding motif of Cap, markedly reduced the phosphorylation of PKC-δ and impeded the recruitment of p-PKC-δ and Cap protein to the nuclear membrane, resulting in a markedly weakened replication and pathogenesis of PCV2 *in vivo*. These findings offer some new insights into the mechanisms of circoviral nuclear egress.

RESULTS

p32 is necessary for the nuclear egress of PCV2. p32 has been reported to mediate and regulate many biological processes during viral infection, including viral gene expression, DNA replication, viral nuclear egress, viral assembly, viral release, and antiviral immune regulation (25–31, 33, 34). To determine the role of p32 in the infection of circovirus, we used PCV2 infection as a model to explore the effects of p32 deficiency on PCV2 replication. We first constructed *p32* gene knockout PK-15 (porcine kidney 15 cell line) cells by using the CRISPR/Cas9 genomic editing system; three guide RNAs, i.e., gRNA-22, gRNA-155, and gRNA-173, were designed to target three respective sites located on exon 1 of the pig *p32* gene. The gRNA-22-derived cell clone (22PK$^{p32-/-}$) and gRNA-155-derived cell clone (155PK$^{p32-/-}$) showed a deficiency of p32 expression, while the gRNA-173-derived cell clone (173PK$^{p32+/+}$) did not show any difference from wild-type PK-15 in p32 expression level (Fig. 1A). It should be mentioned that *p32* knockout did not appreciably affect the viability and proliferation of cells (data not shown). When these cell clones were infected with PCV2, the virus yield (intracellular and extracellular) did not exhibit significant differences between these cells within 24 h of infection. However, as viral infection progressed, extracellular virus yield from p32-deficient cells (22PK$^{p32-/-}$ and 155PK$^{p32-/-}$) was lower than that of wild-type PK-15 and 173PK$^{p32+/+}$ cells from 36 hours postinfection (h p.i.) (Fig. 1B), whereas intracellular virus yield in p32-deficient cells (22PK$^{p32-/-}$ and 155PK$^{p32-/-}$) were beginning to reduce relative to that of wild-type PK-15 and 173PK$^{p32+/+}$ cells from 48 h p.i. (Fig. 1C).

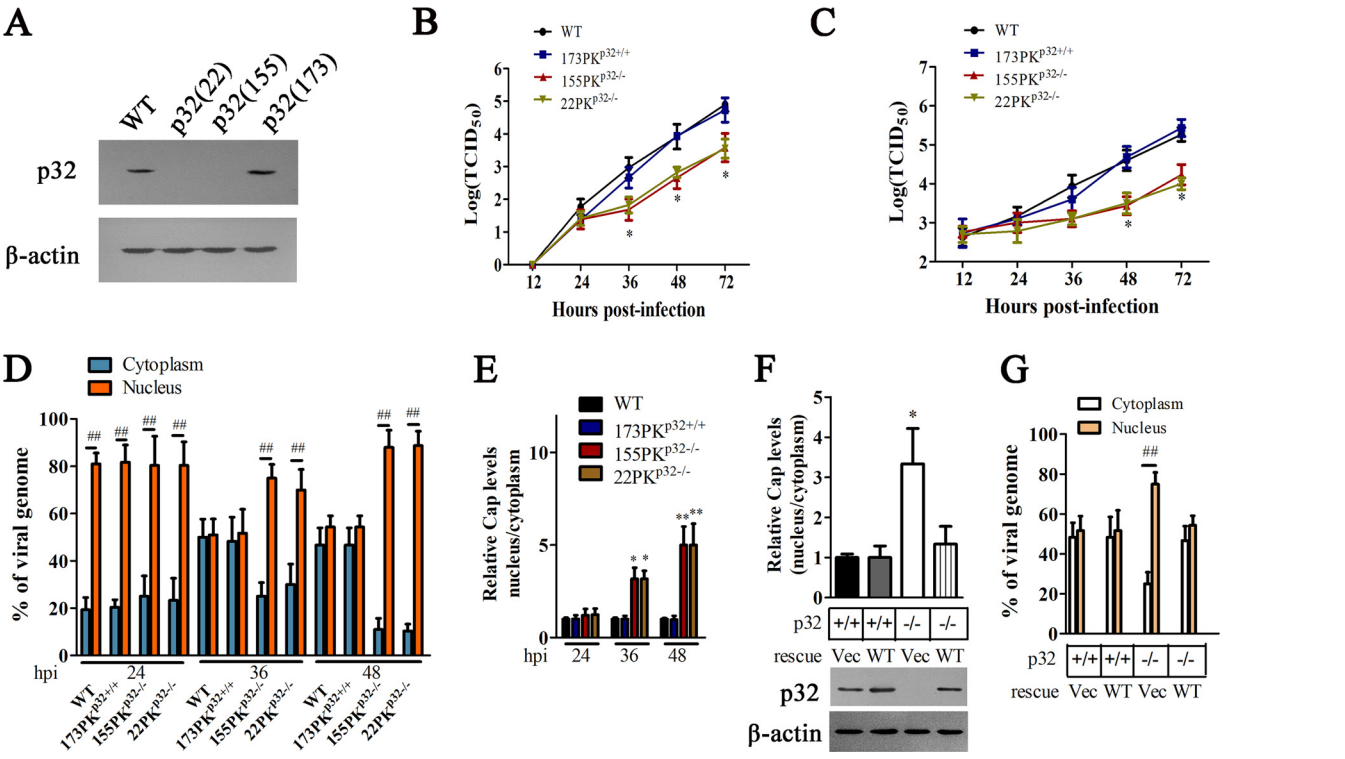

FIG 1 p32 deletion impairs the nuclear egress of PCV2 capsids. (A) Examination of p32 expression in PK-15 cells with a CRISPR/Cas9 system targeting the *p32* locus. Three single-cell clones [p32(22), p32(155), and p32(173)] were derived from cells infected with lentiviral pseudotypes expressing gRNAs 22, 155, and 173, respectively. (B, C) Wild-type PK-15, 22PK$^{p32-/-}$, 155PK$^{p32-/-}$, and 173PK$^{p32+/+}$ cells were infected with PCV2, supernatant and cells were collected at indicated times, and the titers of PCV2 in extracellular (B) and intracellular (C) were detected by 50% tissue culture infective dose (TCID$_{50}$), respectively. *, $P < 0.05$. Comparison were made at the same time points between values in p32 knockout (KO) cells and wild-type PK-15 cells infected by PCV2. (D to E) Depletion of p32 blocks the nuclear egress of PCV2 capsids. Wild-type PK-15, 22PK$^{p32-/-}$, 155PK$^{p32-/-}$, and 173PK$^{p32+/+}$ cells were infected with PCV2 for 24, 36. and 48 h, the proportion of viral DNA copies in cytoplasm and nucleus was measured by quantitative PCR (qPCR) (D), Cap levels were detected by Western blotting, and the relative Cap levels were calculated using ImageJ. (E) The proportion of Cap (nucleus/cytoplasm) is shown (E). *, $P < 0.05$; **, $P < 0.01$. Comparisons were made between values in p32 KO cells and wild-type PK-15 cells infected by PCV2 at the same time points; ##, $P < 0.01$ (compared with the percentage in cytoplasm). (F to G) 22PK$^{p32-/-}$ and 173PK$^{p32+/+}$ cells were transfected with plasmids to express wild-type p32 (WT) or control vector pCI-neo (Vec), respectively, and then the cells were infected with PCV2; after 36 h, the proportions of Cap proteins (nucleus/cytoplasm) (F) and PCV2 DNA in nucleus or cytoplasm (G) were measured. *, $P < 0.05$ (compared with 173PK$^{p32+/+}$ cells transfected with Vec); ##, $P < 0.01$ (compared with percentage in cytoplasm).

In order to determine in which step of viral replication p32 deficiency impaired PCV2 yield, we examined and calculated the distribution ratio of PCV2 in nucleus and cytoplasm of wild-type PK-15 cells and p32-deficient cells. At 24 h postinfection of PCV2, over 80% of viral DNA was distributed in nuclear fractions in either wild-type cells or 173PK$^{p32+/+}$ cells, while p32-deficient cells (22PK$^{p32-/-}$ and 155PK$^{p32-/-}$) also showed similar pattern in viral DNA distribution, suggesting that p32 deficiency does not affect the distribution of viral DNA at 24 h p.i. At 36 and 48 h postinfection of PCV2, nearly 50% of viral DNA was distributed in nuclear fractions in either wild-type cells or 173PK$^{p32+/+}$ cells, but more than 70% of viral DNA (at 36 h p.i,) and nearly 85% of viral DNA (at 48 h p.i.) were still distributed in the nucleus in p32-deficient cells (22PK$^{p32-/-}$ and 155PK$^{p32-/-}$) (Fig. 1D). Consistent with the changes in viral DNA, in both wild-type cells and 173PK$^{p32+/+}$ cells, nearly 50% of Cap proteins were distributed in nuclear fractions at all of the detection times (24, 36, and 48 h p.i.), but in p32-deficient cells (22PK$^{p32-/-}$ and 155PK$^{p32-/-}$), Cap proteins located in the nucleus were about 3-fold those in cytoplasm at 36 h p.i., and about 5-fold those in cytoplasm at 48 h p.i., (Fig. 1E). These results demonstrated that cellular p32 deficiency can alter the distribution of PCV2 DNA and Cap proteins in the late phase of PCV2 infection. To further confirm the function of p32 in this process, we investigated whether exogenous expression of p32 could reverse the distribution of viral DNA and Cap protein in p32-deficient cells. Results revealed that the distribution proportion of Cap protein and viral DNA (nucleus/

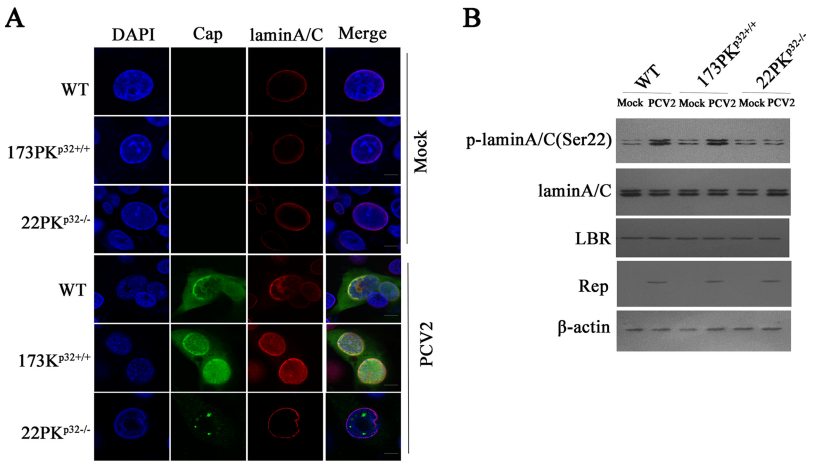

FIG 2 PCV2 infection induces the phosphorylation and redistribution of lamin A/C mediated by p32. (A, B) p32 knockout promoted the redistribution of lamin A/C and reduced the phosphorylation of lamin A/C. Wild-type PK-15, 173PK$^{p32+/+}$, and 22PK$^{p32-/-}$ cells were infected with PCV2, and the redistribution of lamin A/C was determined by laser scanning confocal microscopy (A); the phosphorylation levels of lamin A/C were measured by Western blotting (B).

cytoplasm) in the cells rescued with p32 was similar to that in the p32 wild-type cells (Fig. 1F and G). These results suggested that cellular p32 is important for the nuclear egress of viral particles in PCV2-infected cells.

p32 mediates the phosphorylation of lamin A/C and redistribution of the nuclear lamina during PCV2 infection. Previous studies have showed that the phosphorylation of lamin and redistribution of the nuclear lamina are required for some viral nuclear egress (26, 32, 34). In PCV2-infected wild-type PK-15 and 173PK$^{p32+/+}$ cells, lamin A/C appeared to be diffused from the nuclear rim to nucleoplasm (Fig. 2A), and the phosphorylation levels of lamin A/C (Ser22) were elevated relative to those in mock infection (Fig. 2B). Simultaneously, the distribution of lamin A/C aligned around the nuclear rim in PCV2-infected 22PKp32$^{-/-}$ cells, similar to that in mock-infected cells (Fig. 2A), and the phosphorylation level of lamin A/C (Ser22) remained the same as that in mock-infected wild-type PK-15 cells (Fig. 2B). This was in contrast to wild-type cells, suggesting that p32 is indispensable for phosphorylation of lamin A/C and redistribution of the nuclear lamina during PCV2 infection.

p32 mediates the interaction of lamin A/C, lamin B receptor, and Cap protein. To determine whether Cap protein is the key component in induction of p32 redistribution in PCV2-infected cells, PK-15 cells were transfected with plasmids expressing Flag-p32 and pEGFP-N1 or plasmids expressing Flag-p32 and green fluorescent protein (GFP)-Cap. Confocal microscopy imaging showed that Flag-p32 barely appeared in the nucleus in cells without Cap coexpression but was redistributed from cytoplasm to nucleus, accompanied by GFP-Cap expression (Fig. 3A). These results suggested that Cap plays a critical role in recruitment of p32 to the nucleus during PCV2 infection.

Lamin B receptor (LBR), an integral protein of the INM, has been reported to interact with p32 during the nuclear egress of herpesviruses (26). To further confirm the roles of Cap and p32 in the redistribution of the nuclear lamina induced by PCV2 infection, the possible interactions between lamin A/C, LBR, p32, and Cap protein were analyzed. Coimmunoprecipitation analysis using Cap antibodies showed that Cap interacted with p32, LBR, and lamin A/C in PCV2-infected wild-type PK-15 and 173PK$^{p32+/+}$ cells but not in PCV2-infected 22PK$^{p32-/-}$ cells (Fig. 3B). Meanwhile, coimmunoprecipitation analysis with lamin A/C antibodies showed that lamin A/C interacted with p32, LBR, and Cap in PCV2-infected wild-type PK-15 and 173PK$^{p32+/+}$ cells, but they did not interact with Cap in PCV2-infected 22PK$^{p32-/-}$ cells; lamin A/C did not interact with p32 in cells without PCV2 infection (Fig. 3C). Furthermore, glutathione *S*-transferase (GST) pulldown assay showed that p32 directly interacted with Cap (Fig. 3D) and also directly interacted

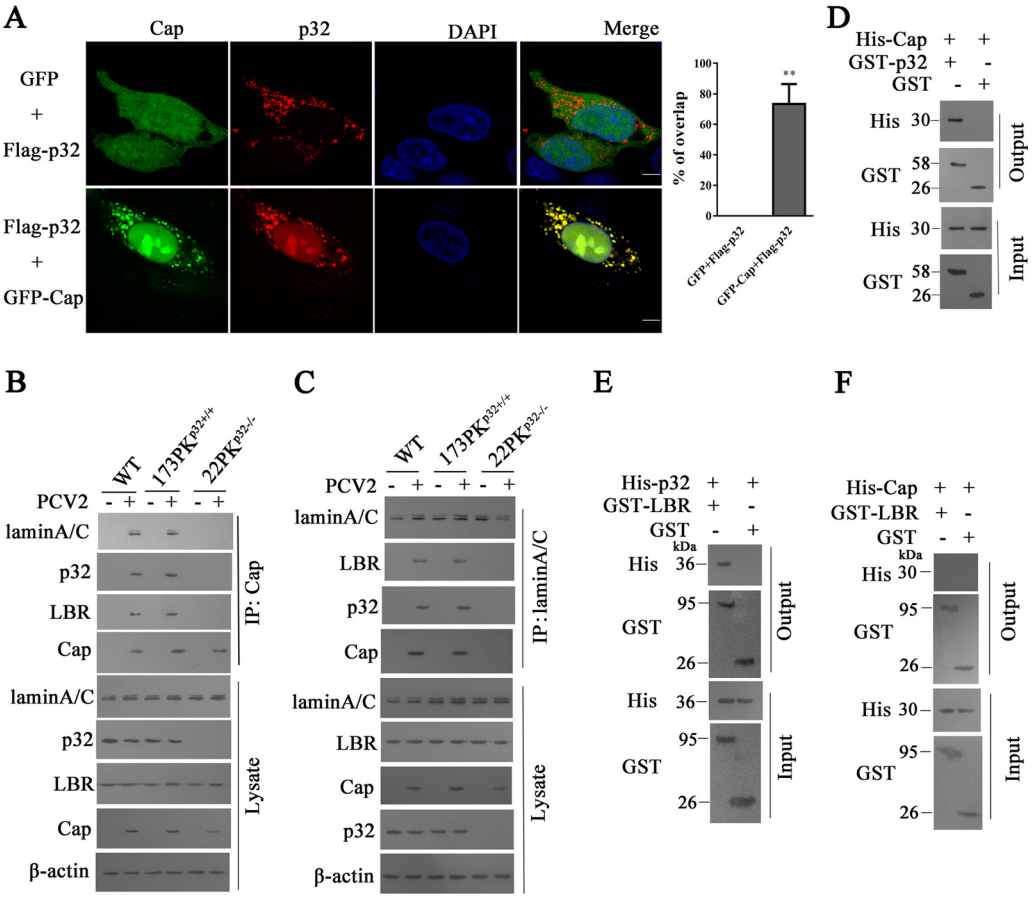

FIG 3 p32 mediated the interaction of lamin A/C, lamin B receptor (LBR), and Cap. (A) PK-15 cells were transfected with pEGFP-Cap and pCI-p32-Flag vectors or with pCI-p32-Flag and pEGFP-N1 vectors; the cells were fixed and subjected to laser scanning confocal microscopy. Images represent the subcellular locations of green fluorescent protein (GFP)-Cap and Flag-p32 proteins (left), and histograms represent the percentage of overlap of Flag-p32 proteins with GFP-Cap, performed using ImageJ software and based on ≥15 cells/sample (right). **, $P < 0.01$ (compared with pCI-p32-Flag and pEGFP-N1 vector cotransfected cells). (B, C) p32 mediates the interaction of lamin A/C, LBR, and Cap protein. Wild-type PK-15, 173PK$^{p32+/+}$, and 22PK$^{p32-/-}$ cells were infected with PCV2, and immunoprecipitation was performed to detect the Cap interaction with lamin A/C, LBR, and p32 using anti-Cap antibodies (B) or anti-lamin A/C antibodies (C). (D to F) Direct interaction of p32 with PCV2 Cap or LBR. Bacterially purified GST-p32 or glutathione *S*-transferase (GST) alone was incubated with purified His-Cap, and proteins bound to glutathione Sepharose beads were analyzed by immunoblotting with the indicated antibodies (D); purified GST-LBR or GST alone was incubated with purified His-p32 (E) or His-Cap (F). Proteins bound to glutathione Sepharose beads were analyzed by immunoblotting with the indicated antibodies.

with LBR, whereas Cap did not appear to directly interact with LBR (Fig. 3E and F). These results suggested that Cap interaction with LBR and lamin A/C is dependent on the presence of p32, and that recruitment of p32 to nucleus by Cap is required for p32 interaction with LBR and lamin A/C in nucleus. In other words, p32 facilitates the formation of a complex on nuclear LBR that provide a platform for phosphorylating lamin A/C to promote the redistribution of lamin A/C. However, it is unclear what phosphorylates lamin A/C in this complex, which requires further investigation.

p32 recruits PKC-δ to the nuclear membrane and phosphorylates lamin A/C during PCV2 infection. PKCs can directly phosphorylate a target protein or indirectly phosphorylate a target protein by activation of downstream kinases (37). PKC-α and PKC-δ have been reported to phosphorylate lamin A/C during viral infection (38). In PCV2-infected PK-15 cells, PKC-δ was phosphorylated at threonine 505 (T505) but not at tyrosine 311 (Y311), whereas PKC-α was not phosphorylated at serine 657 (S657) as was previously reported for Sendai virus (SeV) infection (39) (Fig. 4A). Consistently, at 24, 36 and 48 h post PCV2 infection, the phosphorylation levels of lamin A/C (Ser22) were markedly reduced in cells treated with an inhibitor of PKC-δ isoform (Rottlerin)

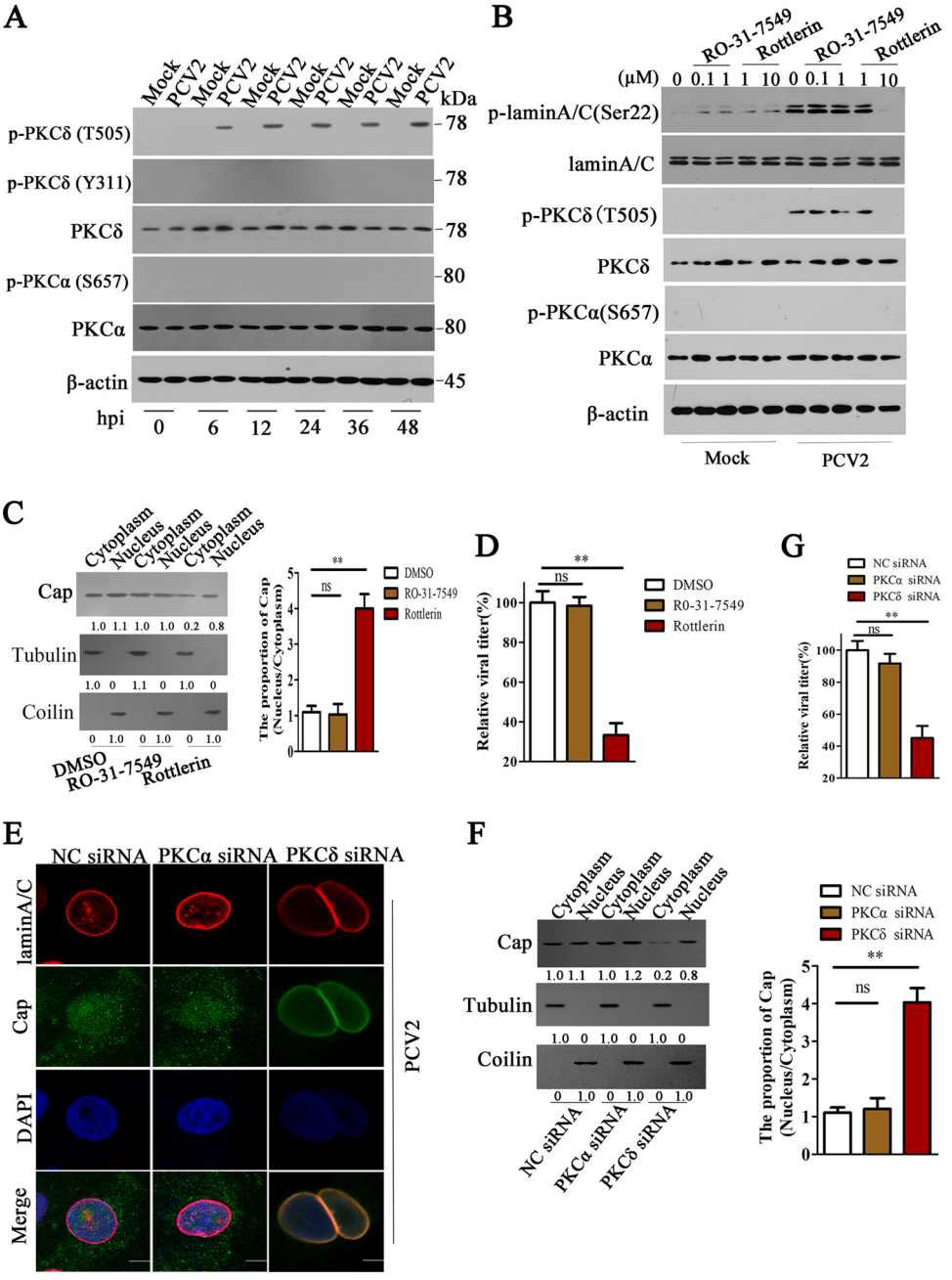

FIG 4 PKC-δ promotes the redistribution of lamin A/C and nuclear egress of PCV2. (A) PK-15 cells were infected with PCV2 or mock-infected for the indicated times, and cell lysates were subjected to immunoblotting using anti-PKC-δ antibody, anti-phospho-PKC-δ (T505), anti-phospho-PKC-δ (Y311), anti-PKC-α antibody, and anti-phospho-PKC-α (S657); β-actin was used as an internal control. The sizes of molecular mass markers (M) are shown in kDa. (B) PKC-δ inhibitor (Rottlerin) impeded the phosphorylation of lamin A/C induced by PCV2. PK-15 cells were treated with inhibitors at different concentrations and harvested at 36 h post PCV2 infection, the phosphorylation levels of lamin A/C (Ser22), PKC-δ (T505), and PKC-α (S657) were detected by immunoblotting. (C, D) PKC-δ inhibitor (Rottlerin) impeded viral nuclear egress and reduced progeny virus production. PK-15 cells were treated with Rottlerin (10 μM), RO-31-7549 (1 μM), or dimethyl sulfoxide (DMSO), as described, for 36 h, and the levels of Cap proteins were detected in nucleus and cytoplasm (C, left). The relative proportion of Cap (nucleus/cytoplasm) was calculated using ImageJ (C, right); the relative viral titers of different inhibitor treatment groups were measured by $TCID_{50}$ (D). **, $P < 0.01$; ns, not significant. (E to G) The knockdown of PKC-δ inhibits the redistribution of lamin A/C, impedes nuclear egress of PCV2 Cap, and reduces the production of PCV2. PK-15 cells were treated with PKC-δ- or PKC-α-specific siRNA 1 and then infected with PCV2. The distribution of lamin A/C was observed using immunofluorescence (E); the levels of Cap proteins in cytoplasm and nucleus were determined by immunoblotting (F, left). The relative proportion of Cap (nucleus/cytoplasm) was calculated (**, $P < 0.01$; ns, not significant); (F, right), the viral production was measured by $TCID_{50}$, and the relative viral titers were calculated (G). **, $P < 0.01$; ns, not significant.

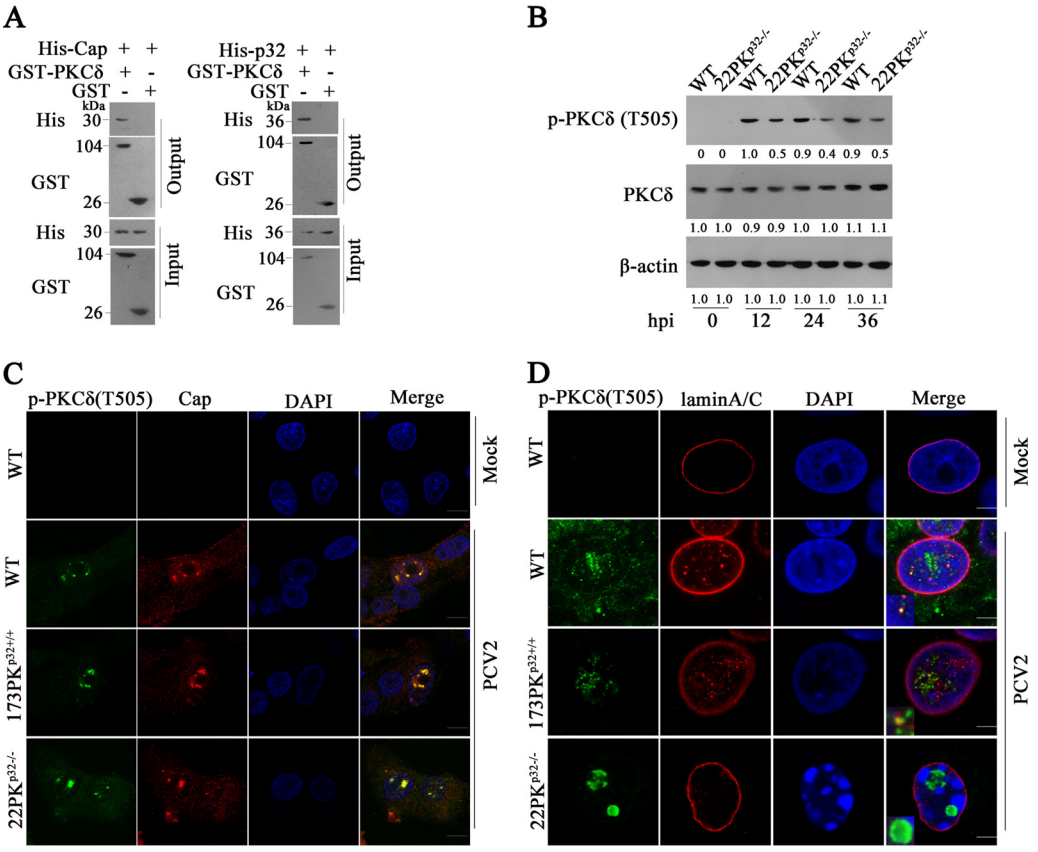

FIG 5 p32 recruits PKC-δ to the nuclear membrane to phosphorylate lamin A/C during PCV2 infection. (A) Direct interaction of PKC-δ with Cap or p32. Purified GST-PKC-δ or GST alone was incubated with purified His-Cap (left panel) or His-p32 (right panel), and proteins bound to glutathione Sepharose beads were analyzed by immunoblotting with the indicated antibodies. (B) Knockout of p32 reduced the phosphorylation levels of PKC-δ (T505). Wild type PK-15 and 22PK$^{p32-/-}$ cells were infected with PCV2, the cell lysates were subjected to immunoblotting using anti-PKC-δ (T505) and PKC-δ antibodies. (C, D) p32 deficiency impeded recruitment of p-PKC-δ to nuclear membrane during PCV2 infection. Wild-type PK-15, 173PK$^{p32+/+}$, and 22PK$^{p32-/-}$ cells were infected with PCV2. The interaction of p-PKC-δ (T505) with Cap (C) or lamin A/C (D) and the distribution of these molecules were observed under laser scanning confocal microscopy.

(data not shown), and the inhibitory effect of Rottlerin on lamin A/C (Ser22) phosphorylation induced by PCV2 infection appeared to be dose dependent (Fig. 4B). However, the phosphorylation level of lamin A/C (Ser22) was not decreased in PCV2-infected cells treated with PKC-α inhibitor (RO-31-7549) compared to that in the PCV2-infected cells without inhibitors (Fig. 4B). These results indicate that PCV2 infection activates PKC-δ at the threonine 505 residue to further promote the phosphorylation of lamin A/C. Consequently, in the presence of Rottlerin, PCV2 infection did not apparently lead to the redistribution of lamin A/C from the nuclear rim to nucleoplasm (data not shown), and the proportion of PCV2 Cap in nucleus and cytoplasm was upregulated about 4-fold compared with cells without Rottlerin treatment (Fig. 4C); this resulted in dramatically decreased progeny PCV2 production (Fig. 4D). Similarly, the specific small interfering RNA (siRNA) of PKC-δ blocked the redistribution of lamin A/C, increased the proportion of PCV2 in nucleus, and eventually limited the production of progeny virus (Fig. 4E to G). These results demonstrated that PCV2 infection activates PKC-δ to phosphorylate lamin A/C and disassemble the nuclear lamina so as to promote the nuclear egress of viruses.

To further interrogate the roles of Cap and p32 in the phosphorylation of PKC-δ, we assessed if PKC-δ directly interacted with Cap and p32. The GST pulldown results showed that PKC-δ could directly bind to PCV2 Cap protein and p32 (Fig. 5A). Next, we investigated the effects of p32 deficiency on the activation, translocation and function of PKC-δ. In both wild-type and p32$^{-/-}$ cells, PCV2 infection increased PKC-δ expression

and induced phosphorylation of PKC-δ at T505 (Fig. 5B). However, the phosphorylation level of PKC-δ was decreased by half in p32$^{-/-}$ cells relative to that in wild-type cells during PCV2 infection (Fig. 5B), suggesting that although p32 is not indispensable for the expression and phosphorylation of PKC-δ, p32 can further promote the activation of PKC-δ in PCV2-infected cells. In most PCV2-infected wild-type PK-15 and 173PK$^{p32+/+}$ cells, p-PKC-δ was colocalized with Cap in the nuclear membrane and diffused along with lamin A/C (Fig. 5C and D). However, in all PCV2-infected 22PK$^{p32-/-}$ cells, p-PKC-δ and Cap were colocalized in the center of nucleoplasm and aggregated into a punctum; almost no cells displayed a colocalization of p-PKC-δ and Cap in the nuclear membrane, and cells barely exhibited a diffused p-PKC-δ along with lamin A/C (Fig. 5C and D). These results indicated that p32 deficiency impedes recruitment of p-PKC-δ to nuclear membrane during PCV2 infection.

PLC, together with ERK1/2 and JNK signaling pathways, promotes the activation of PKC-δ during PCV2 infection. The PKC signaling pathway, which involves phospholipid-dependent serine/threonine kinases, can cross talk with a wide spectrum of signal transduction pathways in response to a variety of stimuli (40–42). To investigate how PKC-δ is activated during PCV2 infection, we first explored the roles of PI3K/Akt, PLC, Jun N-terminal protein kinase (JNK), p38-mitogen-activated protein kinase (MAPK), and extracellular signal-regulated kinase (ERK) signaling pathways in the activation of PKC-δ. The results showed that a PLC inhibitor (U73122) significantly inhibited the phosphorylation levels of PKC-δ at both 6 h p.i. and 36 h p.i.; an ERK inhibitor (PD98059) and a JNK inhibitor (SP6000125) attenuated PKC-δ phosphorylation at 36 h p.i., but not at 6 h p.i. Of note, PI3K/Akt inhibitor LY294002 and p38 MAPK inhibitor SB203580 did not have any effect on PKC-δ phosphorylation at either 6 h p.i. or 36 h p.i. (data not shown). Consistent with the characteristic effects of inhibitors on PKC-δ phosphorylation induced by PCV2, downregulation of JNK1 and ERK1 by specific siRNAs also had similar effects characteristic of PCV2-induced PKC-δ phosphorylation (Fig. 6A). Meanwhile, blocking diacylglycerol (DAG) also decreased the phosphorylation levels of PKC-δ at 6 h p.i. and 36 h p.i. (Fig. 6B). In line with the changes in PKC-δ phosphorylation, addition of PLC inhibitor (U73122), ERK inhibitor (PD98059), JNK inhibitor (SP6000125), and DAG antagonist (1-hexadecyl-2-acetyl glycerol [HAG]), or treatment with the specific siRNAs of JNK1 and ERK1, significantly inhibited the phosphorylation and redistribution of lamin A/C, whereas PI3K/Akt and p38 MAPK inhibitors or their specific siRNAs did not affect the phosphorylation and redistribution of lamin A/C in PCV2-infected cells (Fig. 6C to E; micrographs data not shown). As a result, treatment with PLC, ERK, and JNK inhibitors or the specific siRNAs of JNK1 and ERK1, significantly increased the proportion of PCV2 Cap in nucleus (Fig. 6F) and eventually limited the production of progeny virus (Fig. 6G). These results suggested that PCV2 can activate PLC to promote PKC-δ phosphorylation via intracellular DAG in the early phase of infection (6 h p.i.), and further activates ERK and JNK signaling pathways that enhance the PKC-δ phosphorylation, likely through intracellular DAG or another unknown signaling pathway in the late phase of infection (36 h p.i.).

The N-terminal three continuous arginine residues of PCV2 Cap are crucial for binding to p32. Our above results suggested that p32, as a Cap-binding protein, is crucial for the nuclear egress of PCV2. To identify the key region and amino acid residues of Cap that are required for interacting with p32, we first tested the interaction of full-length porcine p32 (Flag-tagged) with ten deletion mutants of Cap that we previously constructed (43). A coimmunoprecipitation assay showed that Cap fragments 1 to 41, 1 to 83, 1 to 107, and 1 to 161 interacted with porcine p32, along with the full-length Cap, whereas Cap fragments 42 to 234, 78 to 234, 118 to 234, 162 to 234, and 199 to 234 were not able to interact with porcine p32, suggesting that the N-terminal residues 1 to 41 are responsible for the interaction of Cap with p32 (Fig. 7A). Further experiments showed that fragment 21 to 41 was responsible for binding p32, whereas fragment 1 to20 was not (Fig. 7B). Consistent with the results of coimmunoprecipitation assay, confocal immunofluorescence (IF) microscopy analyses showed that Cap fragments 1 to 41, 1 to 83, 1 to 107, 1 to 161, and 21 to 41 were colocalized

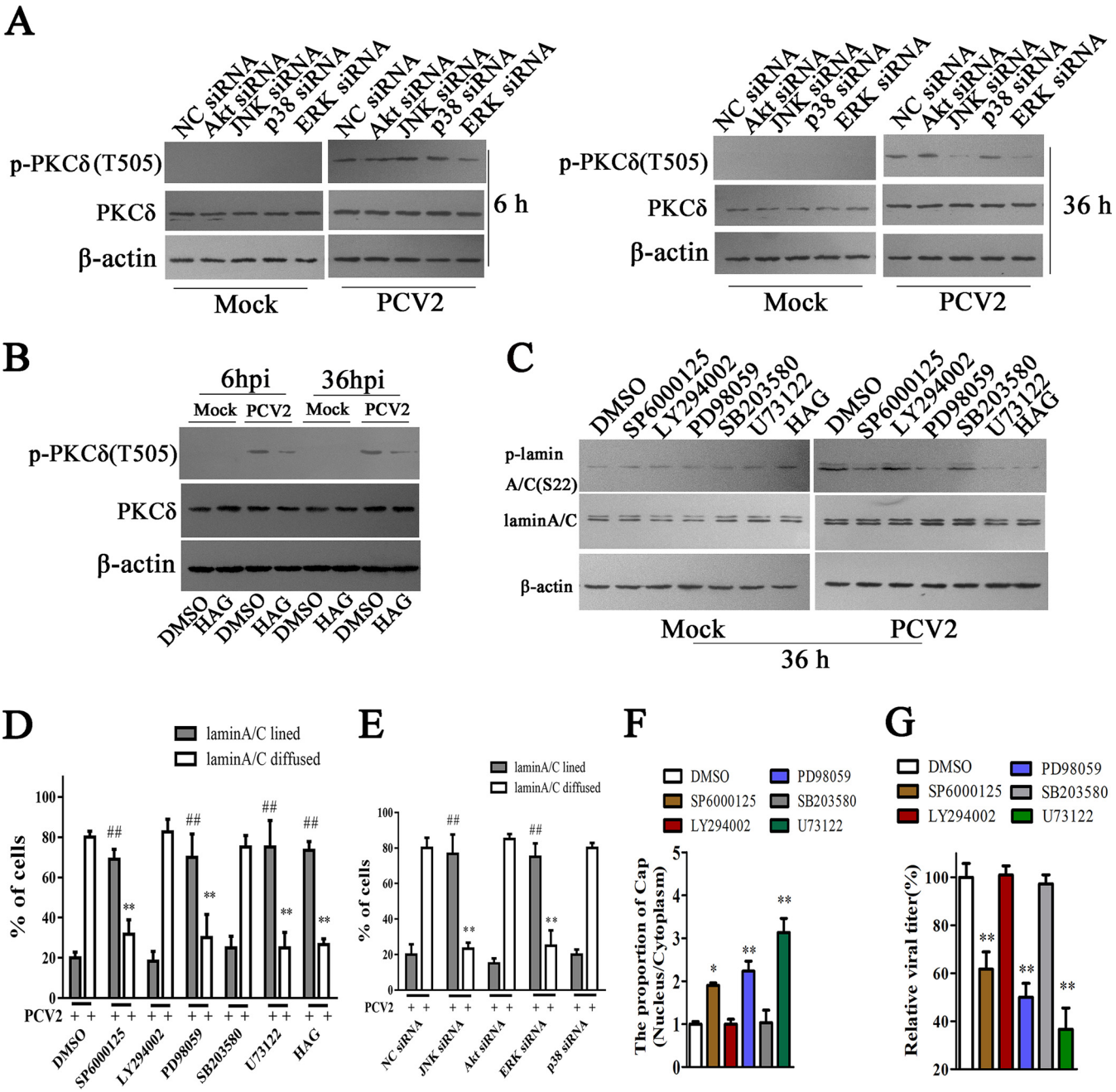

FIG 6 PLC, along with the ERK1/2 and JNK1/2 signaling pathways, promotes the phosphorylation of lamin A/C and the nuclear egress of PCV2. (A) PK-15 cells were transfected with indicated siRNAs for 36 h, and then the cells were infected with PCV2 for 6 h and 36 h and the phosphorylation of PKC-δ(T505) was detected by immunoblotting. (B) 1-Hexadecyl-2-acetyl glycerol (HAG) can inhibit the phosphorylation of PKC-δ. PK-15 cells were pretreated with HAG for 2 h, the cells were infected with PCV2 for 6 h and 36 h, and the phosphorylation of PKC-δ (T505) was detected by immunoblotting. (C, D) PK-15 cells were treated with indicated inhibitors, the phosphorylation of lamin A/C was detected by immunoblotting (C), and the distribution of lamin A/C was determined by immunofluorescence at 36 h post PCV2 infection; the percentages of cells displaying aligned lamin A/C or diffuse lamin A/C were calculated (D), **, $P < 0.01$; ##, $P < 0.01$ (compared with DMSO-treated cells). (E) PK-15 cells were treated with indicated siRNAs for 36 h, the distribution of lamin A/C was determined by immunofluorescence at 36 h post PCV2 infection, and the percentages of cells displaying aligned lamin A/C or diffuse lamin A/C were calculated, **, $P < 0.01$; ##, $P < 0.01$ (compared with negative-control [NC] siRNA-transfected cells). (F, G) PK-15 cells were treated with indicated inhibitors, the levels of Cap proteins were detected in the proteins extracted from nucleus and cytoplasm, and the relative proportion of Cap (nucleus/cytoplasm) was calculated using ImageJ (F). The viral production was measured by $TCID_{50}$, and the relative viral titers were calculated (G). *, $P < 0.05$; **, $P < 0.01$ (compared with DMSO-treated cells).

with p32, whereas Cap fragments 42 to 234, 78 to 234, 118 to 234, 162 to 234, 199 to 234, and 1 to 20 were not (data not shown).

To further identify the amino acids in the N terminus (amino acids [aa] 21 to 41) of Cap responsible for this binding, we analyzed the primary sequence of Cap protein.

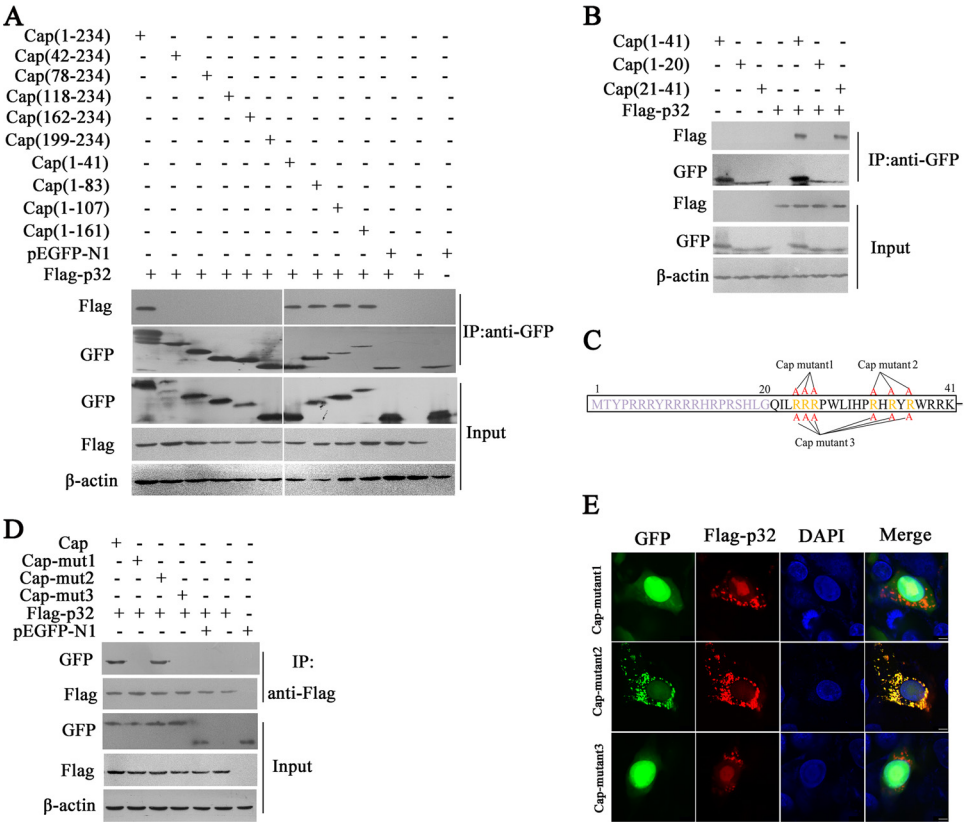

FIG 7 Cap binds to p32 via its N-terminal 24RRR26. (A) Cap fragment (aa 1 to 41) interacted with p32. HEK293T cells were cotransfected with plasmids encoding full-length Cap or deletion mutants fused with a GFP tag, along with Flag-p32; cell lysates were immunoprecipitated with an anti-GFP antibody and immunoblotted using indicated antibodies. (B) The Cap N-terminal aa residues 21 to 41 interacted with p32. HEK293T cells were cotransfected with plasmids encoding the N-terminal aa residues 1 to 41, 1 to 20, or 21 to 41 fused with a GFP tag, along with Flag-p32; cell lysates were immunoprecipitated with anti-GFP antibody, followed by immunoblotting using indicated antibodies. (C) The Cap mutants were constructed with arginine residues at residues 24 to 26, 33, 35, and 37 replaced with alanine. (D) Mapping the crucial amino acids of Cap responsible for Cap/p32 interaction. HEK293T cells were cotransfected with Cap or Cap mutants 1, 2, and 3, along with Flag-p32 expression vectors, and the cell lysates were subjected to immunoprecipitation and immunoblotting using the indicated antibodies. (E) Confirmation by immunofluorescence assay of the crucial amino acids of PCV2 Cap that interact with p32. PK-15 cells were cotransfected with plasmids indicated in panel D and subjected to confocal microscopy observation at 36 h posttransfection. These results were confirmed in three independent experiments.

Since p32 is an acidic protein, we screened for basic amino acid residues within the N-terminal aa 21 to 41 of Cap and constructed two three-arginine mutants, i.e., Cap mutant 1 (–24RRR26– replaced with –24AAA26–) and Cap mutant 2 (–33R-35R-37R –replaced with –33A-35A-37A–), as well as a six-arginine Cap mutant 3 (–24RRR26– and –33R-35R-37R– simultaneously replaced with –24AAA26– and –33A-35A-37A–). Mutant sites in this region (aa 21 to 41) are noted in Fig. 7C. When these mutant constructs were cotransfected with Flag-p32 into HEK293T cells, coimmunoprecipitation assay showed that Cap mutant 1 and Cap mutant 3 failed to bind Flag-p32, but Cap mutant 2 was still able to bind to Flag-p32 (Fig. 7D). Consist with this observation, confocal microscopy analysis showed that only Cap mutant 2 was colocalized with Flag-p32 (Fig. 7E). These results demonstrated that residues 24RRR26 in the N terminus of Cap are crucial for PCV2 Cap binding to p32.

Sequence alignment of PCV2 different genotypes (PCV2a, PCV2b, PCV2c, PCV2d, and PCV2e) Cap proteins revealed that the arginine residues 24RRR26 are absolutely conserved (Fig. 8A to E). Furthermore, sequence alignment of PCV1, PCV2, and PCV3 Cap proteins revealed that arginine residues 24RRR26 are also absolutely conserved (Fig. 8F and G). Meanwhile, sequence alignment of Cap of different circovirus species showed that two strains (canine circovirus strain XF16 and feather disease virus isolate

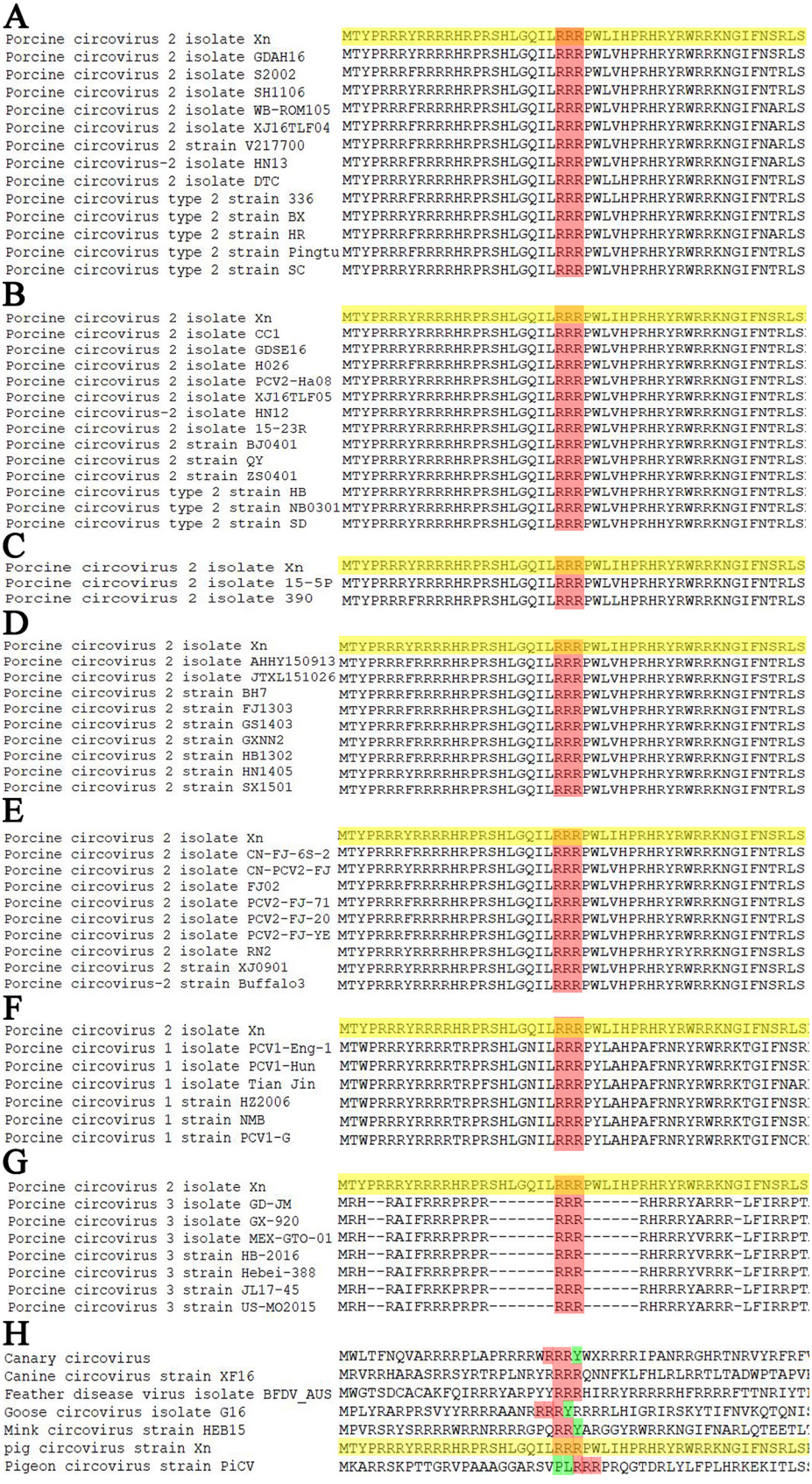

FIG 8 Alignment of amino acid sequences of Cap in N-terminal 24RRR26 and adjacent amino acid sequences. (A) Alignment of PCV2b isolate Xn (GenBank accession number MH492006) and the strains of genotype PCV2a.

(Continued on next page)

BFDV_AUS) were also 100% identical to our strain (porcine circovirus type 2 Xn) in the 24RRR26 residues; other circovirus strains also harbor some continuous arginine motifs in a nearby region (Fig. 8H). These analyses further revealed that the N-terminal three-continuous-arginine motif of Cap proteins is conserved among circovirus species, which might explain in part its essential role in binding p32 and in circoviral nuclear egress.

Mutation of 24RRR26 of Cap protein impedes the replication and pathogenesis of PCV2. To assess whether Cap N-terminal 24RRR26 is crucial for the replication and pathogenesis of PCV2, we first constructed a PCV2 mutant strain (PCV2RmA) in which arginine residues (24 to 26) of Cap were replaced by alanine (AAA) and then tested progeny virion production in wild-type PK-15 cells. As might be expected, progeny virion production in PCV2RmA-infected cells were significantly lower than that of wild type PCV2-infected cells (Fig. 9A). In PCV2RmA-infected cells, p32 was localized in the cytoplasm, and PCV2RmA Cap was not colocalized with p32 (data not shown); the proportion (Cap in cytoplasm/Cap in nucleus) of Cap protein in PCV2RmA-infected cells was lower than that in wild-type PCV2-infected cells (Fig. 9B). Simultaneously, the distribution of lamin A/C presented linearly in nuclear membranes of most PCV2RmA-infected cells, which was different from the diffused lamin A/C distribution in most wild-type PCV2-infected cells (Fig. 9C). p-PKC-δ was colocalized with mutated Cap, either in cytoplasm or nucleoplasm, in PCV2RmA-infected cells but not in the nuclear membrane of infected cells (data not shown); the phosphorylation levels of lamin A/C and PKC-δ were reduced in PCV2RmA-infected cells compared with those in PCV2-infected cells (Fig. 9D).

Since the PCV2 detected in the above study is PCV2b, in order to assess whether Cap N-terminal 24RRR26 residues are crucial for the nuclear egress of other genotype PCV2 strains, we constructed PCV2a, PCV2c, PCV2d, and PCV2e mutants (PCV2aRmA, PCV2cRmA, PCV2dRmA, and PCV2eRmA) in which arginine residues (24 to 26) of Cap were replaced by alanine (AAA), and then examined and calculated the distribution ratio of these PCV2 strains in the nucleus and cytoplasm of cells. Results showed that the proportion (nucleus/cytoplasm) of viral DNA in PCV2RmA mutants-infected cells was higher than that in wild-type PCV2 (a, c, d, and e)-infected cells (Fig. 9E); and progeny virion production in PCV2RmA mutant-infected cells was significantly lower than that in wild-type PCV2-infected cells (Fig. 9F).

Next, we explored whether three continuous arginine substitutions affect the replication and pathogenesis of PCV2 *in vivo*. To this end, we tested viral load in serum and tissues, the Cap protein levels, and pathological lesions in different tissues of PCV2RmA-infected piglets and compared them with those of wild-type PCV2-infected piglets (note that the genotype of both PCV2 and PCV2RmA is PCV2b). Results showed that viral load in serum of PCV2RmA-infected piglets was significantly lower than that in wild-type PCV2-infected piglets at 7 to 28 days postinfection (dpi) (Fig. 9G). Consistent with this, in lung and lymph node tissues, the Cap levels of PCV2RmA-infected piglets were significantly lower than those of PCV2-infected piglet at 28 dpi (Fig. 9H). Consequently, PCV2RmA infection induced more light histological lesions in the lung and lymph node tissues than did the wild-type PCV2 (Fig. 9I). PCV2RmA-infected piglets showed mild interstitial pneumonia (characterized by slightly thickened alveolus walls) relative to wild-type PCV2-infected piglets; lymphoid depletion (characterized by lymphocytes necrosis in both the cortex and paracortex and decreasing or lacking lymphocytes) was easily observed in wild-type PCV2-infected piglets but not in PCV2RmA-

FIG 8 Legend (Continued)
(B) Alignment of PCV2b isolate Xn and the strains of genotype PCV2b. (C) Alignment of PCV2b isolate Xn and the strains of genotype PCV2c. (D) Alignment of PCV2b isolate Xn and the strains of genotype PCV2d. (E) Alignment of PCV2b isolate Xn and the strains of genotype PCV2e. (F) Alignment of PCV2b isolate Xn and the strains of porcine circovirus type 1. (G) Alignment of PCV2b isolate Xn and the strains of porcine circovirus type 3. (H) Alignment of porcine circovirus type 2 isolate Xn and different circovirus species strains. The red highlights represent arginine, the yellow highlights represent the sequence of porcine circovirus type 2 isolate Xn, and the green highlights represent nonarginine residues.

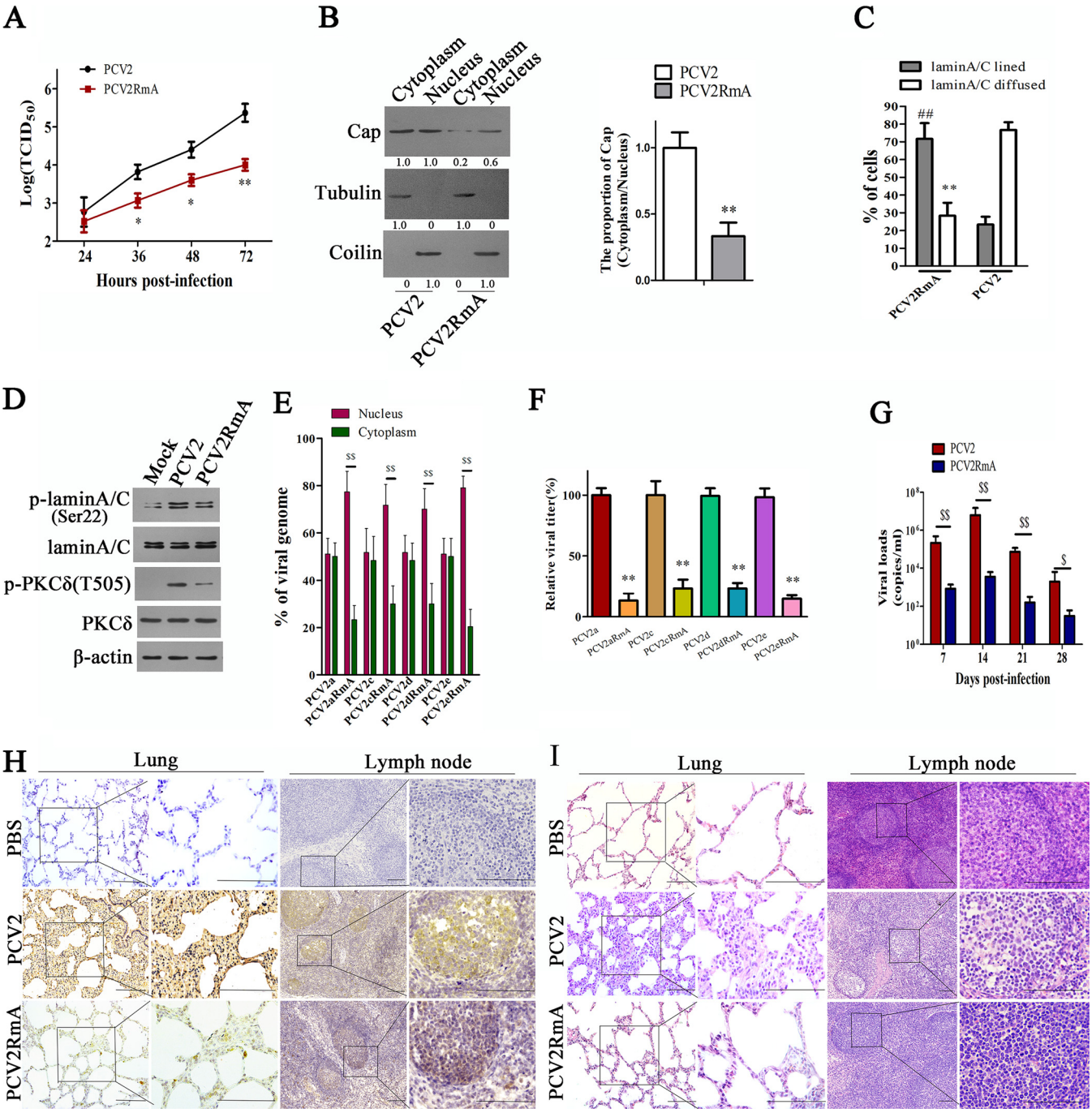

FIG 9 Mutation of Cap 24RRR26 residues diminishes the replication and pathogenesis of PCV2. (A, B) PCV2 mutant (PCV2RmA) with RRR residues (aa 24 to 26) being replaced by alanine showed reduced viral production and nuclear egress. PK-15 cells were infected with PCV2 or PCV2RmA, and viral titers (A) and the viral Cap levels in nucleus and cytoplasm (B) were measured and calculated. *, $P < 0.05$; **, $P < 0.01$ (compared with PCV2-infected cells at the same time point). (C, D) PCV2RmA infection resulted in reduced redistribution of lamin A/C and limited p-PKC-δ redistribution to nuclear membrane. PK-15 cells were infected with PCV2 or PCV2RmA, the distribution of lamin A/C were assayed by immunofluorescence, and the percentages of cells displaying aligned lamin A/C or diffused lamin A/C were calculated (C), **, $P < 0.01$; ##, $P < 0.01$ (compared with PCV2-infected cells); the phosphorylation of lamin A/C and p-PKC-δ(T505) were detected by immunoblotting (D). (E–F) Different PCV2 genotype mutants with RRR residues (aa 24 to 26) being replaced by alanine showed an increased proportion (nucleus/cytoplasm) of viral DNA and reduced progeny virion production. PK-15 cells were infected with PCV2 (PCV2a, PCV2c, PCV2d, or PCV2e) or PCV2RmA mutants (PCV2aRmA, PCV2cRmA, PCV2dRmA, or PCV2eRmA) for 36 h, and the proportion of viral DNA copies in cytoplasm and nucleus was measured by qPCR. $$, $P < 0.01$ (E); the relative viral titers of supernatant were measured by $TCID_{50}$. **, $P < 0.01$ (compared with wild-type PCV2-infected cells) (F). (G) Piglets were infected by intranasal injection with PCV2 or PCV2RmA. The viral genomic numbers in serum at the indicated times were measured by qPCR. $, $P < 0.05$; $$, $P < 0.01$. (H, I) Representative images of immunohistochemistry (IHC) staining for PCV2 using Cap antibody (H) and hematoxylin and eosin (H&E) staining (I) in lung and lymph node derived from PCV2-, PCV2RmA-, or PBS-challenged groups. Bar, 100 μm.

TABLE 1 Comparison of histological lesion scores of lung and lymph node from PCV2- and PCV2RmA-infected piglets

		Histological lesion score	
Group[a]	Piglet label	Lung[b]	Lymph nodes[c]
PBS	A	0	0
	B	0	0
	C	0	0
	D	0	0
	E	0	0
PCV2	F	5	3
	G	4	2
	H	4	3
	I	5	2
	J	3	2
PCV2RmA	K	1	1
	L	2	1
	M	1	1
	N	3	2
	O	2	1

[a]PBS; phosphate-buffered saline; PCV2, porcine circovirus type 2; PCV2RmA, a PCV2 mutant.
[b]Score ranges from 0 (normal) to 6 (severe).
[c]Score ranges from 0 (normal) to 3 (severe).

infected piglets (Fig. 9I). The mean lung histological lesion scores and mean lymphoid depletion scores in the PCV2RmA infection group were significantly lower than those in the wild-type PCV2 infection group (Table 1). Taken together, these results indicated that mutation of 24RRR26 of the Cap protein impedes the replication and pathogenesis of PCV2.

DISCUSSION

p32, as a multiligand-binding, multicompartmental, and multifunctional protein, has been reported to mediate viral nuclear egress through binding to viral proteins (26, 33, 35). Although previous studies have indicated that p32 can facilitate HSV-1 nuclear egress through interaction with HSV-1 ICP34.5 and UL47 to regulate the rearrangement of the nuclear lamina (25, 26), the exact roles of p32 in phosphorylation and rearrangement of lamin A/C remain undefined. In our present study, we have found that p32 serves as a cargo or adaptor to transport PCV2 nucleocapsids into nuclear membrane and to recruit p-PKC-δ to the nuclear membrane, the latter of which phosphorylates lamin A/C, resulting in the rearrangement of nuclear lamina and thus facilitating PCV2 nuclear egress.

The NE consists of an INM and an ONM (4, 44). The ONM is continuous and functionally interrelated with the rough endoplasmic reticulum, while the INM contains a set of membrane proteins that provide anchoring sites for chromatin and lamins. The nuclear lamina is a highly stable, filamentous scaffold structure underneath the INM, consisting mainly of lamin types A/C and B, which maintains nuclear shape and mechanical stability (45). However, for virus infection, the nuclear lamina potentially presents a barrier to block the transit of virus capsids from the nucleus to the cytoplasm (38). Therefore, phosphorylation-driven disassembly and rearrangement of the nuclear lamina are involved in the process of some viral infections (33, 46–48). HSV-1, HSV-2, murine cytomegalovirus (MCMV), HCMV, and Epstein-Barr virus (EBV) use similar mechanisms to disrupt the nuclear lamina to facilitate the release of virions from the nucleus (49). The phosphorylation of lamin A/C on serine 22 residues has been shown to be crucial for disassembly of the nuclear lamina (50). In some virus-infected cells, the phosphorylated levels of lamin A/C are upregulated (38, 50), promoting disassembly of nuclear lamina, which in turn permits nucleocapsids to gain access to the inner nuclear membrane for the subsequent steps of nuclear egress (50). We have found that the phosphorylated levels of lamin A/C serine 22 were also markedly increased in PCV2-

infected cells, which resulted in the disassembly of nuclear lamina. This was in contrast to p32-deficient cells, in which the level of phosphorylated lamin A/C Ser22 was not increased by PCV2 infection, with lamin A/C still aligning around the nuclear rim as in uninfected cells. These findings indicated that p32 is indispensable for the nuclear egress of PCV2. In intracellular signaling networks activated by PCV2, p32 can act as a bridge to facilitate the formation of a complex on nuclear LBR that provides a platform for the phosphorylation of lamin A/C to promote the redistribution of lamin A/C during porcine circoviral nuclear egress. These findings supported the notion that PCV2 infection promotes phosphorylation of lamin A/C accompanied by disassembly of the nuclear lamina, both of which are dependent on p32.

In the viral nuclear egress process, nuclear membrane-associated viral proteins, together with viral or cellular kinases, normally form a "nuclear egress complex" that facilitates nuclear lamina disassembly and transit of new virions from the nucleus (51). For the nuclear egress complex, recruitment of cellular and/or virus-encoded protein kinases to nuclear lamins is crucial for the site-specific phosphorylation of nuclear lamins and lamin-binding proteins (32, 50). Previous studies have shown that cellular PKC and viral proteins can phosphorylate the nuclear lamins. For instance, in HSV-1-infected cells, in addition to cellular protein kinases PKC-δ, Us3, a serine/threonine kinase of HSV-1, is involved in phosphorylation of lamin A/C to disassemble the nuclear lamina (26, 38). In HCMV-infected cells, cellular PKC-α and viral kinase pUL97 are recruited to the nuclear rim to directly phosphorylate lamin A/C, inducing nuclear lamina disassembly to promote viral nuclear egress (32, 34). For PCV2, the unique structure protein, Cap, is not a kinase, which suggests that a host kinase must be recruited to the nuclear rim to phosphorylate lamin A/C. Indeed, we found that in PCV2-infected cells, PKC-δ (threonine 505) was activated and was involved in the phosphorylation of lamin A/C Ser 22, whereas PKC-α was not implicated in this process. Intriguingly, viral infection can recruit distinct PKC isoforms into the nucleus via different signaling pathways; for instance, HSV-1 recruits PKC-δ (26), HCMV recruits PKC-α (34), and MCMV recruits Ca-dependent PKC (48). In our study, we discovered that PCV2 infection resulted in recruiting PKC-δ. Importantly, p32 deficiency markedly reduced the phosphorylation of PKC-δ and impeded the recruitment of p-PKC-δ and Cap protein to the nuclear membrane. In some physiological processes or viral infection processes, members of the protein kinase C family are activated in response to different stimuli or second messengers (38, 52, 53). Our studies have shown that the phosphorylation of threonine 505 on PKC-δ is essential for its action in the phosphorylation of lamin A/C. Furthermore, our study demonstrated that threonine phosphorylation of PKC-δ was regulated by the PLC, ERK, and JNK signaling pathways, with the ERK and JNK pathways likely acting to coordinate the activation of PKC-δ and lamin A/C and the nuclear egress of PCV2. Thus, we observed that the generation of progeny PCV2 was regulated by the PLC/PKC-δ signaling pathway together with ERK and JNK signaling.

A previous study has reported that aa 1 to 59 of PCV-2b Cap mediate the interaction with p32 (54). Here, we further confirmed that PCV2 Cap 24 to 26 RRR is required for the interaction of Cap with p32. Mutation of the 24-RRR-26 of Cap protein abolished the ability of Cap protein to bind to p32. Notably, the 24 to 26 arginine residues of Cap are absolutely conserved among PCV1, PCV2, and PCV3, and the 24 26 arginine residues of porcine circoviral Cap had higher identity with other circovirus species, such as canine circovirus and feather disease virus strains. These analyses implied that the Cap proteins of different circovirus species likely possess the same important function to bind to p32 protein through the same amino acid motif. Our results demonstrated that p-PKC-δ could not be recruited to the nuclear membrane in cells when PCV2 Cap was mutated (PCV2RmA). Notably, the PCV2b mutant progeny with the three-arginine-residue (aa 24 to 26) mutation in the Cap protein showed markedly reduced progeny virus production and milder histological lesions in infected piglets than wild-type PCV2. Simultaneously, since p32 deficiency limits the nuclear egress of circovirus and further blocks the replication of viral genomic DNA in the latter phase, the total amount of Cap in the *p32*-knockout cell lines appears to be substantially less than that in wild-type PK-15

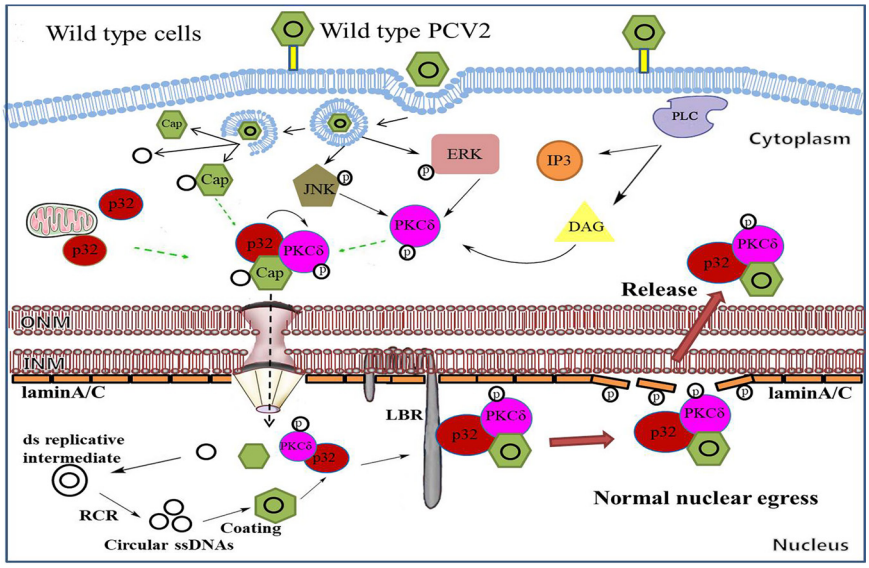

FIG 10 Model of PCV2 nuclear egress. PCV2 infection promotes the phosphorylation of PKC-δ via PLC-mediated signaling at the early infection phase, which is further amplified by JNK and ERK1/2 signaling at the late infection phase. In wild-type cells, Cap recruits p32 and phosphorylates PKC-δ (p-PKC-δ), and this leads to transport of p32 and p-PKC-δ into the nucleus. In the nucleus, p32, as an adaptor, further recruits p-PKC-δ and Cap to the nuclear membrane via binding with LBR to phosphorylate lamin A/C, which promotes the rearrangement of nuclear lamina and facilitates viral nuclear egress.

cells. All of these data demonstrate that p32 is utilized by PCV2 to enhance its replication.

In summary, the data presented in this work demonstrate that, at the late phase of PCV2-infection, p32 is employed by PCV2 to enhance the phosphorylation of PKC-δ, which is subsequently recruited to the nuclear membrane and phosphorylation of lamin A/C; this led to rearrangement of nuclear lamina, thus facilitating PCV2 nuclear egress (Fig. 10). In p32-deficient cells, PCV2 infection can promote the phosphorylation of PKC-δ, but Cap and p-PKC-δ are not able to traffic to the nuclear membrane, thus abolishing the phosphorylation of lamin A/C and nuclear lamina rearrangement and impairing the nuclear egress of PCV2. Similarly, a PCV2 mutant (PCV2RmA), a mutated PCV2 whose mutated Cap loses the ability to bind p32, is not able to transported p32 into the nucleus, thus abolishing the phosphorylation of lamin A/C and nuclear lamina rearrangement and limiting the rearrangement of nuclear lamina and viral nuclear egress. Taken together, our findings offer detailed mechanisms of PCV2 nuclear egress and will help us to further understand the pathogenic mechanisms of PCV2.

MATERIALS AND METHODS

Reagents and cells. Monoclonal mouse anti-green fluorescent protein (anti-GFP) (catalog number CSB-MA000051M0m) was purchased from Cusabio; rabbit monoclonal anti-GFP antibody (catalog number G10362), rabbit monoclonal anti-Flag antibody (catalog number 701629), mouse monoclonal anti-Flag antibody (catalog number MA1-91878), horseradish peroxidase (HRP)-conjugated anti-mouse IgG (catalog number 31430), and anti-rabbit IgG (catalog number 31460) were purchased from Thermo Fisher; rabbit monoclonal anti-p32 antibody (catalog number 6502), rabbit anti-PKC-α antibody (catalog number 2056), rabbit monoclonal anti-PKC-δ antibody (catalog number 9616), rabbit phospho-PKC-δ (Thr505) antibody (catalog number 9374), rabbit phospho-PKC-δ (Y311) antibody (catalog number 2055), and rabbit monoclonal phospho-lamin A/C (Ser22) antibody (catalog number 13448) were purchased from Cell Signaling Technology; mouse monoclonal anti-p32 antibody was purchased from Hycult Biotech (catalog number HM2014); rabbit monoclonal anti-phospho-PKC-α (S657) antibody (catalog number 180848) and rabbit monoclonal anti-lamin B receptor antibody (catalog number 32535) were purchased from Abcam; fluorescein isothiocyanate (FITC)-conjugated goat anti-rabbit IgG antibody (catalog number BA1105) was purchased from Boster; and DyLight 594-conjugated goat anti-mouse IgG antibody (catalog number JC-PB007HD) was purchased from Jing Cai. Protein G-agarose, protein A-agarose, PKC-α inhibitor (R0-31-7549) and PKC-δ inhibitor (Rottlerin) were purchased from Santa Cruz; PI3K/Akt inhibitor

(LY294002), ERK1/2 MAPK inhibitor (PD98059), and p38 MAPK inhibitor (SB203580) were purchased from Merck; JNK inhibitor SP6000125, PLC inhibitor (U73122), protease inhibitor tail, and HAG (which blocks diacylglycerol) were purchased from Sigma; and minute cytoplasmic and nuclear extraction kits for cells (catalog number SC-003) was purchased from Invent Biotechnologies.

HEK 293T (human embryonic kidney 293 cells transfected with SV40 large T-antigen) cells were purchased from the American Type Culture Collection (ATCC); PK-15 (porcine kidney 15 cell line) cells were donated from the innovative team of animal pathogen surveillance and epidemiology at the Harbin Veterinary Research Institute, Chinese Academy of Agricultural Sciences (CAAS). These cells were cultured in Dulbecco's modified Eagle medium (DMEM; Invitrogen) supplemented with 10% heat-inactivated fetal bovine serum (FBS; HyClone) in a 5% CO_2 culture.

Plasmids. PCV2 open reading frame 2 (ORF2) and nine deletion mutant fragments were constructed as described in our previous study (43). Three Cap site-directed mutants (Cap mutant 1, Cap mutant 2, and Cap mutant 3), as described in the Results, were constructed into a pEGFP vector by overlap PCR. The porcine *p32* gene was amplified from PK-15 cells and then was subcloned into the pCI-neo vector with Flag tag. Moreover, the *p32* gene and Cap were subcloned into the pET-28a vector. The porcine *pkc-δ* gene was amplified from PK-15 cells and then subcloned into the pGEX-4T-1 vector; all sequences were confirmed by sequencing analysis (Sangon Biotech).

CRISPR/Cas9-mediated *p32* deletion. To generate *p32* knockout cells, we used CRISPR/Cas9 methodology (43, 55). Briefly, three guide RNAs (gRNAs) encoding sequences (sg#1-ACGGCGGTGCCCAGGGC GCG, sg#2-GGGCTCCTGAGCGTGCGTGC, and sg#3-GCCGGGTCGGTGCAGCCGCC) designed to target the corresponding sequences of p32 genomic loci were cloned into the BsmB I sites of the Lenti-CRISPRv2 plasmid (catalog number 52961; Addgene). The recombinant vectors were transfected into HEK293T cells together with psPAX2 (catalog number 12260; Addgene) and pMD2.G (catalog number 12259; Addgene) to package lentiviral particles. Then, PK-15 cells were infected with recombinant lentiviruses and selected with 5 μg/ml puromycin (InvivoGen) to obtain p32-deficient cells. The selected single clone cells were cultured and checked by Western blotting and sequencing.

IF confocal microscopy. Cells were grown on the coverslips in 24-well culture plates and transfected with indicated plasmids or infected with virus for the indicated time. Cells were fixed with 4% paraformaldehyde for 20 min at room temperature and permeabilized with 0.1% TritonX-100 for 15 min at room temperature. Cells were washed with 0.1 M phosphate-buffered saline (PBS) and were further preincubated with 2% bovine serum albumin for 1 h at 37°C. Then, cells were successively incubated with primary antibodies overnight and with secondary antibodies for 1 h at 37°C, followed by thrice washing as described above. After quick staining with 4,6-diamidino-2-phenylindole (DAPI; Sigma-Aldrich), coverslips were mounted onto glass slides in the presence of fluorescence mounting medium. Samples were analyzed by Leica TCS SP8 laser scanning confocal microscope. Images were recorded using Leica X software.

RNA interference. Specific siRNAs were designed to silence Akt1, JNK1, ERK1, p38 MAPK, PKC-α, and PKC-δ. The sequences of siAkt1, siERK1, and sip38 were referred to in our previous study (56); JNK1, PKC-α, and PKC-δ siRNAs were designed (JNK1, AAAGAAUGUCUUACCUUCU; PKC-δ 1, GCUGCCAUCCAC AAGAAAU; PKC-δ 2, GCAUGAACGUGCACCAUAA; PKC-δ 3, GGGCCUCGCUGUCUGU CAA; PKC-α 1, CCAA UCGUUUCGCCCGCAA, PKC-α 2, GGGACCGAACAA CAAGG AA; PKC-α 3, GCCUCCGUUUGAU GGCGAA) in this study. The effects of siRNAs were identified by Western blotting. Cells were transfected with specific siRNAs or negative-control (NC) siRNA using Lipofectamine 3000 (Invitrogen), and then cells were grown at 37°C for 24 to 48 h and subsequently infected with PCV2 for 36 h. The cells were collected and used to perform relevant assays.

Coimmunoprecipitation and Western blotting. These methods were performed as in a previous study (43). In detail, the cells cultured in a 100-mm-diameter dish (Thermo Fisher) were transfected with indicated plasmids using Lipofectamine 3000; 36 h later, the cells were lysed with lysis buffer (150 mM NaCl, 50 mM Tris-HCl [pH 7.4], 1% Nonidet P-40, 0.5% TritonX-100, 1 mM EDTA, 0.1% sodium deoxycholate, 1 mM dithiothreitol, 0.2 mM phenylmethylsulfonyl fluoride, and a protease inhibitor protease inhibitor cocktail [Sigma-Aldrich]) on ice for 30 min. The cell lysate supernatant was collected by centrifuging and was then precleared by incubation with protein G/protein A agarose for 1 h at 4°C. The supernatant was incubated with indicated antibodies for overnight at 4°C and incubated again with protein G agarose/protein A agarose for 30 min at room temperature. Then, protein G agarose/protein A agarose was centrifuged at 2,000 $\times$ *g* for 10 s, and washed three times with PBS. Finally, the bound proteins were eluted by boiling for 10 min in 2$\times$ loading buffer, followed by SDS-PAGE and immunoblotting. The process of immunoblotting was performed as described in in detail a previous study (43). Immunoreactive bands were visualized using enhanced chemiluminescence (ECL) reagents (Bio-Rad).

Cell fractionation. Infected cells were briefly treated with trypsin-EDTA and gently resuspended in DMEM, then centrifuged for 5 min at 3,000 $\times$ *g* and washed with PBS. After completely aspirating the PBS, 200 μl of nuclear isolation buffer (1.28 M sucrose, 40 mM Tris-HCl [pH 7.5], 20 mM $MgCl_2$, and 4% TritonX-100), 200 μl PBS, and 600 μl water were added to each sample, the pellets were gently resuspended, and placed on ice for 20 min. Samples were centrifuged at 2,500 $\times$ *g* for 15 min. Supernatants (cytoplasmic fractions) were collected, and then the pellets (nuclear fraction) were gently resuspended in 500 μl 0.1 M PBS. Both the cytoplasmic and nuclear fractions were processed following the viral extraction protocol recommended by the manufacturer.

The construction of PCV2 and PCV2 mutants. Wild-type PCV2 strain (genotype PCV2b; GenBank accession number MH492006) was isolated and stocked in our lab. To construct a PCV2b mutant strain (PCV2RmA), primers were designed in which arginine residues (24 to 26) encoding nucleotides of Cap were replaced by alanine (AAA)-encoding nucleotides, and then genes of the PCV2b mutant were

amplified from wild-type PCV2 genomes by overlap PCR. The PCV2b mutant progeny virions were produced in wild-type PK-15 cells and used in the animal experiments in this study.

The genomic DNAs of PCV2 (PCV2a, PCV2c, PCV2d, and PCV2e) were constructed by gene synthesis; in PCV2RmA mutants, the encoding nucleotides of arginine residues (24 to 26) were replaced with the nucleotides encoding alanine (AAA), and the PCV2 and PCV2RmA mutant progeny virions were produced in wild-type PK-15 cells. The GenBank accession numbers of PCV2a, PCV2c, PCV2d, and PCV2e are KF871067, EU148504, MG833033, and MF589523, respectively.

Animal experiment. Fifteen 5-week-old piglets, free of PCV2, porcine reproductive and respiratory syndrome virus, classical swine fever virus, pseudorabies virus, porcine parvovirus, swine influenza virus, and *Mycoplasma hyopneumoniae* infection, were randomly assigned to 3 groups of 5 piglets each and housed separately. The pigs in group 1 were inoculated with 1×10^6 50% tissue culture infective dose ($TCID_{50}$) of PCV2. Those in group 2 were each inoculated with 1×10^6 $TCID_{50}$ of PCV2RmA. The pigs in group 3 were inoculated with PBS for a negative control. Postchallenge, pigs were monitored for 28 days for rectal temperatures and clinical signs. Blood were collected from all animals on 0, 7, 14, 21, and 28 days postinfection (dpi) for detection of PCV2 using real-time PCR.

Ethics statement. All animal experiments were approved by the Institutional Animal Care and Use Committee (IACUC) of Northwest A&F University (permit numbers 20161112 and 20170516) and were performed according to the Animal Ethics Procedures and Guidelines of the People's Republic of China. No other specific permissions were required for these activities. This study did not involve endangered or protected species.

Pathological examination. Necropsies of piglets were performed at 28 dpi, and superficial inguinal lymph node, lung, liver, heart, spleen, kidney, brain, and stomach tissues were collected. Samples were then fixed by 10% formalin, embedded in paraffin wax, sliced in a microtome (Leica) to 4 μm, and affixed onto the slides, followed by hematoxylin and eosin (HE) staining for microscopic examination and immunohistochemistry (IHC) staining for PCV2 infection detection (57).

Statistical analysis. Data are expressed as mean $\pm$ standard error of the mean (SEM) (standard deviation [SD]). Statistical analyses were performed with GraphPad Prism 5 software. Immunofluorescence values were calculated using Image-Pro Plus 6.0. A P value of <0.05 was considered significant.

ACKNOWLEDGMENTS

We thank the teachers of the Life Science Research Core Service (LSRCS) for assistance with immunofluorescence.

This work was supported by the National Natural Science Foundation of China (grants 31672535, 31872447, and 31972686 to Y.H. and D.T.) and by U.S. NIH grants 1R01AI112381 and 1R21AI109464 to S.-L.L. This work was also supported by the Key R&D Program of Shaanxi Province (grants 2018ZDCXL-NY-02-07 and 2018ZDCXL-NY-02-04) and by Fundamental Research Funds for the Central Universities (grant 2452017023).

REFERENCES

1. Schmid M, Speiseder T, Dobner T, Gonzalez RA. 2014. DNA virus replication compartments. J Virol 88:1404–1420. https://doi.org/10.1128/JVI.02046-13.
2. Whittaker GR, Helenius A. 1998. Nuclear import and export of viruses and virus genomes. Virology 246:1–23. https://doi.org/10.1006/viro.1998.9165.
3. And HK, Nakanishi A. 1998. How do animal DNA viruses get to the nucleus? Annu Rev Microbiol 52:627. https://doi.org/10.1146/annurev.micro.52.1.627.
4. Johnson DC, Baines JD. 2011. Herpesviruses remodel host membranes for virus egress. Nat Rev Microbiol 9:382–394. https://doi.org/10.1038/nrmicro2559.
5. Hofemeister H, O'Hare P. 2008. Nuclear pore composition and gating in herpes simplex virus-infected cells. J Virol 82:8392–8399. https://doi.org/10.1128/JVI.00951-08.
6. Blondot ML, Bruss V, Kann M. 2016. Intracellular transport and egress of hepatitis B virus. J Hepatol 64:S49–S59. https://doi.org/10.1016/j.jhep.2016.02.008.
7. Ohkawa T, Welch MD. 2018. Baculovirus actin-based motility drives nuclear envelope disruption and nuclear egress. Curr Biol 28:2153–2159.E4. https://doi.org/10.1016/j.cub.2018.05.027.
8. Roller RJ, Baines JD. 2017. Herpesvirus nuclear egress. Adv Anat Embryol Cell Biol 223:143–169. https://doi.org/10.1007/978-3-319-53168-7_7.
9. Zhang X, Xu K, Wei D, Wu W, Yang K, Yuan M. 2017. Baculovirus infection induces disruption of the nuclear lamina. Sci Rep 7:7823. https://doi.org/10.1038/s41598-017-08437-5.
10. Feng M, Kong X, Zhang J, Xu W, Wu X. 2018. Identification of a novel host protein SINAL10 interacting with GP64 and its role in *Bombyx mori* nucleopolyhedrovirus infection. Virus Res 247:102–110. https://doi.org/10.1016/j.virusres.2018.02.005.
11. Zhao Y, Zheng H, Xu A, Yan D, Jiang Z, Qi Q, Sun J. 2016. Analysis of codon usage bias of envelope glycoprotein genes in nuclear polyhedrosis virus (NPV) and its relation to evolution. BMC Genomics 17:677. https://doi.org/10.1186/s12864-016-3021-7.
12. Maroto B, Valle N, Saffrich R, Almendral JM. 2004. Nuclear export of the nonenveloped parvovirus virion is directed by an unordered protein signal exposed on the capsid surface. J Virol 78:10685–10694. https://doi.org/10.1128/JVI.78.19.10685-10694.2004.
13. Todd D. 2004. Avian circovirus diseases: lessons for the study of PMWS. Vet Microbiol 98:169–174. https://doi.org/10.1016/j.vetmic.2003.10.010.
14. Schoemaker NJ, Dorrestein GM, Latimer KS, Lumeij JT, Kik MJ, van der Hage MH, Campagnoli RP. 2000. Severe leukopenia and liver necrosis in young African grey parrots (*Psittacus erithacus erithacus*) infected with psittacine circovirus. Avian Dis 44:470–478. https://doi.org/10.2307/1592565.
15. Phenix KV, Weston JH, Ypelaar I, Lavazza A, Smyth JA, Todd D, Wilcox GE, Raidal SR. 2001. Nucleotide sequence analysis of a novel circovirus of canaries and its relationship to other members of the genus *Circovirus* of the family *Circoviridae*. J Gen Virol 82:2805–2809. https://doi.org/10.1099/0022-1317-82-11-2805.
16. Smyth JA, Weston J, Moffett DA, Todd D. 2001. Detection of circovirus infection in pigeons by *in situ* hybridization using cloned DNA probes. J Vet Diagn Invest 13:475–482. https://doi.org/10.1177/104063870101300604.
17. Li L, McGraw S, Zhu K, Leutenegger CM, Marks SL, Kubiski S, Gaffney P,

Dela Cruz FN, Jr, Wang C, Delwart E, Pesavento PA. 2013. Circovirus in tissues of dogs with vasculitis and hemorrhage. Emerg Infect Dis 19:534–541. https://doi.org/10.3201/eid1904.121390.
18. Segales J, Allan GM, Domingo M. 2005. Porcine circovirus diseases. Anim Health Res Rev 6:119–142. https://doi.org/10.1079/AHR2005106.
19. Lian H, Liu Y, Li N, Wang Y, Zhang S, Hu R. 2014. Novel circovirus from mink, China. Emerg Infect Dis 20:1548–1550. https://doi.org/10.3201/eid2009.140015.
20. Opriessnig T, Meng XJ, Halbur PG. 2007. Porcine circovirus type 2 associated disease: update on current terminology, clinical manifestations, pathogenesis, diagnosis, and intervention strategies. J VET Diagn Invest 19:591–615. https://doi.org/10.1177/104063870701900601.
21. Ha Z, Xie CZ, Li JF, Wen SB, Zhang KL, Nan FL, Zhang H, Guo YC, Wang W, Lu HJ, Jin NY. 2018. Molecular detection and genomic characterization of porcine circovirus 3 in pigs from Northeast China. BMC Vet Res 14:321. https://doi.org/10.1186/s12917-018-1634-6.
22. Stenzel T, Dziewulska D, Muhire BM, Hartnady P, Kraberger S, Martin DP, Varsani A. 2018. Recombinant goose circoviruses circulating in domesticated and wild geese in Poland. Viruses 10:107. https://doi.org/10.3390/v10030107.
23. Song T, Hao J, Zhang R, Tang M, Li W, Hui W, Fu Q, Wang C, Xin S, Zhang S, Rui P, Ren H, Ma Z. 2019. First detection and phylogenetic analysis of porcine circovirus type 2 in raccoon dogs. BMC Vet Res 15:107. https://doi.org/10.1186/s12917-019-1856-2.
24. Finsterbusch T, Steinfeldt T, Doberstein K, Rodner C, Mankertz A. 2009. Interaction of the replication proteins and the capsid protein of porcine circovirus type 1 and 2 with host proteins. Virology 386:122–131. https://doi.org/10.1016/j.virol.2008.12.039.
25. Liu Z, Kato A, Oyama M, Kozuka-Hata H, Arii J, Kawaguchi Y. 2015. Role of host cell p32 in herpes simplex virus 1 de-envelopment during viral nuclear egress. J Virol 89:8982–8998. https://doi.org/10.1128/JVI.01220-15.
26. Wang Y, Yang Y, Wu S, Pan S, Zhou C, Ma Y, Ru Y, Dong S, He B, Zhang C, Cao Y. 2014. p32 is a novel target for viral protein ICP34.5 of herpes simplex virus type 1 and facilitates viral nuclear egress. J Biol Chem 289:35795–35805. https://doi.org/10.1074/jbc.M114.603845.
27. Luo Y, Yu H, Peterlin BM. 1994. Cellular protein modulates effects of human immunodeficiency virus type 1 Rev. J Virol 68:3850–3856.
28. Berro R, Kehn K, de la Fuente C, Pumfery A, Adair R, Wade J, Colberg-Poley AM, Hiscott J, Kashanchi F. 2006. Acetylated Tat regulates human immunodeficiency virus type 1 splicing through its interaction with the splicing regulator p32. J Virol 80:3189–3204. https://doi.org/10.1128/JVI.80.7.3189-3204.2006.
29. Matthews DA, Russell WC. 1998. Adenovirus core protein V interacts with p32—a protein which is associated with both the mitochondria and the nucleus. J Gen Virol 79:1677–1685. https://doi.org/10.1099/0022-1317-79-7-1677.
30. Kittlesen DJ, Chianese-Bullock KA, Yao ZQ, Braciale TJ, Hahn YS. 2000. Interaction between complement receptor gC1qR and hepatitis C virus core protein inhibits T-lymphocyte proliferation. J Clin Invest 106:1239–1249. https://doi.org/10.1172/JCI10323.
31. Van Scoy S, Watakabe I, Krainer AR, Hearing J. 2000. Human p32: a coactivator for Epstein-Barr virus nuclear antigen-1-mediated transcriptional activation and possible role in viral latent cycle DNA replication. Virology 275:145–157. https://doi.org/10.1006/viro.2000.0508.
32. Milbradt J, Auerochs S, Sticht H, Marschall M. 2009. Cytomegaloviral proteins that associate with the nuclear lamina: components of a postulated nuclear egress complex. J Gen Virol 90:579–590. https://doi.org/10.1099/vir.0.005231-0.
33. Marschall M, Marzi A, Aus Dem Siepen P, Jochmann R, Kalmer M, Auerochs S, Lischka P, Leis M, Stamminger T. 2005. Cellular p32 recruits cytomegalovirus kinase pUL97 to redistribute the nuclear lamina. J Biol Chem 280:33357–33367. https://doi.org/10.1074/jbc.M502672200.
34. Milbradt J, Auerochs S, Marschall M. 2007. Cytomegaloviral proteins pUL50 and pUL53 are associated with the nuclear lamina and interact with cellular protein kinase C. J Gen Virol 88:2642–2650. https://doi.org/10.1099/vir.0.82924-0.
35. Changotra H, Turk SM, Artigues A, Thakur N, Gore M, Muggeridge MI, Hutt-Fletcher LM. 2016. Epstein-Barr virus glycoprotein gM can interact with the cellular protein p32 and knockdown of p32 impairs virus. Virology 489:223–232. https://doi.org/10.1016/j.virol.2015.12.019.
36. Robles-Flores M, Rendon-Huerta E, Gonzalez-Aguilar H, Mendoza-Hernandez G, Islas S, Mendoza V, Ponce-Castaneda MV, Gonzalez-Mariscal L, Lopez-Casillas F. 2002. p32 (gC1qBP) is a general protein kinase C (PKC)-binding protein; interaction and cellular localization of P32-PKC complexes in ray hepatocytes. J Biol Chem 277:5247–5255. https://doi.org/10.1074/jbc.M109333200.
37. Mondal A, Dawson AR, Potts GK, Freiberger EC, Baker SF, Moser LA, Bernard KA, Coon JJ, Mehle A. 2017. Influenza virus recruits host protein kinase C to control assembly and activity of its replication machinery. Elife 6:e26910. https://doi.org/10.7554/eLife.26910.
38. Wu S, Pan S, Zhang L, Baines J, Roller R, Ames J, Yang M, Wang J, Chen D, Liu Y, Zhang C, Cao Y, He B. 2016. Herpes simplex virus 1 induces phosphorylation and reorganization of lamin A/C through the $\gamma_1$34.5 protein that facilitates nuclear egress. J Virol 90:10414–10422. https://doi.org/10.1128/JVI.01392-16.
39. Maharaj NP, Wies E, Stoll A, Gack MU. 2012. Conventional protein kinase C-alpha (PKC-alpha) and PKC-beta negatively regulate RIG-I antiviral signal transduction. J Virol 86:1358–1371. https://doi.org/10.1128/JVI.06543-11.
40. Dempsey EC, Newton AC, Mochly-Rosen D, Fields AP, Reyland ME, Insel PA, Messing RO. 2000. Protein kinase C isozymes and the regulation of diverse cell responses. Am J Physiol Lung Cell Mol Physiol 279:L429–L438. https://doi.org/10.1152/ajplung.2000.279.3.L429.
41. Mackay K, Mochly-Rosen D. 2001. Localization, anchoring, and functions of protein kinase C isozymes in the heart. J Mol Cell Cardiol 33:1301–1307. https://doi.org/10.1006/jmcc.2001.1400.
42. Nishizuka Y. 1995. Protein kinase C and lipid signaling for sustained cellular responses. FASEB J 9:484–496. https://doi.org/10.1096/fasebj.9.7.7737456.
43. Wang T, Du Q, Wu X, Niu Y, Guan L, Wang Z, Zhao X, Liu SL, Tong D, Huang Y. 2018. Porcine MKRN1 modulates the replication and pathogenesis of PCV2 by inducing capsid protein ubiquitination and degradation. J Virol 92:e00100-18. https://doi.org/10.1128/JVI.00100-18.
44. Shimi T, Butin-Israeli V, Goldman RD. 2012. The functions of the nuclear envelope in mediating the molecular crosstalk between the nucleus and the cytoplasm. Curr Opin Cell Biol 24:71–78. https://www.ncbi.nlm.nih.gov/pubmed/22192274.
45. Broers JL, Ramaekers FC, Bonne G, Yaou RB, Hutchison CJ. 2006. Nuclear lamins: laminopathies and their role in premature ageing. Physiol Rev 86:967–1008. https://doi.org/10.1152/physrev.00047.2005.
46. Reynolds AE, Liang L, Baines JD. 2004. Conformational changes in the nuclear lamina induced by herpes simplex virus type 1 require genes U(L)31 and U(L)34. J Virol 78:5564–5575. https://doi.org/10.1128/JVI.78.11.5564-5575.2004.
47. Lee CP, Huang YH, Lin SF, Chang Y, Chang YH, Takada K, Chen MR. 2008. Epstein-Barr virus BGLF4 kinase induces disassembly of the nuclear lamina to facilitate virion production. J Virol 82:11913–11926. https://doi.org/10.1128/JVI.01100-08.
48. Hamirally S, Kamil JP, Ndassa-Colday YM, Lin AJ, Jahng WJ, Baek MC, Noton S, Silva LA, Simpson-Holley M, Knipe DM, Golan DE, Marto JA, Coen DM. 2009. Viral mimicry of Cdc2/cyclin-dependent kinase 1 mediates disruption of nuclear lamina during human cytomegalovirus nuclear egress. PLoS Pathog 5:e1000275. https://doi.org/10.1371/journal.ppat.1000275.
49. Lee CP, Chen MR. 2010. Escape of herpesviruses from the nucleus. Rev Med Virol 20:214–230. https://doi.org/10.1002/rmv.643.
50. Milbradt J, Hutterer C, Bahsi H, Wagner S, Sonntag E, Horn AH, Kaufer BB, Mori Y, Sticht H, Fossen T, Marschall M. 2016. The prolyl isomerase Pin1 promotes the herpesvirus-induced phosphorylation-dependent disassembly of the nuclear lamina required for nucleocytoplasmic egress. PLoS Pathog 12:e1005825. https://doi.org/10.1371/journal.ppat.1005825.
51. Cibulka J, Fraiberk M, Forstova J. 2012. Nuclear actin and lamins in viral infections. Viruses 4:325–347. https://doi.org/10.3390/v4030325.
52. Murugappan S, Shankar H, Bhamidipati S, Dorsam RT, Jin J, Kunapuli SP. 2005. Molecular mechanism and functional implications of thrombin-mediated tyrosine phosphorylation of PKCdelta in platelets. Blood 106:550–557. https://doi.org/10.1182/blood-2004-12-4866.
53. Hall KJ, Jones ML, Poole AW. 2007. Coincident regulation of PKCdelta in human platelets by phosphorylation of Tyr311 and Tyr565 and phospholipase C signalling. Biochem J 406:501–509. https://doi.org/10.1042/BJ20070244.
54. Kouokam Fotso GB, Bernard C, Bigault L, de Boisseson C, Mankertz A, Jestin A, Grasland B. 2016. The expression level of gC1qR is down regulated at the early time of infection with porcine circovirus of type 2 (PCV-2) and gC1qR interacts differently with the Cap proteins of porcine circoviruses. Virus Res 220:21–32. https://doi.org/10.1016/j.virusres.2016.04.006.

55. Tan R, Nakajima S, Wang Q, Sun H, Xue J, Wu J, Hellwig S, Zeng X, Yates NA, Smithgall TE, Lei M, Jiang Y, Levine AS, Su B, Lan L. 2017. Nek7 protects telomeres from oxidative DNA damage by phosphorylation and stabilization of TRF1. Mol Cell 65:818–831.E5. https://doi.org/10.1016/j.molcel.2017.01.015.
56. Du Q, Wu X, Wang T, Yang X, Wang Z, Niu Y, Zhao X, Liu SL, Tong D, Huang Y. 2018. Porcine circovirus type 2 suppresses IL-12p40 induction via capsid/gC1qR-mediated microRNAs and signalings. J Immunol 201:533–547. https://doi.org/10.4049/jimmunol.1800250.
57. Sorden SD, Harms PA, Nawagitgul P, Cavanaugh D, Paul PS. 1999. Development of a polyclonal-antibody-based immunohistochemical method for the detection of type 2 porcine circovirus in formalin-fixed, paraffin-embedded tissue. J Vet Diagn Invest 11:528–530. https://doi.org/10.1177/104063879901100607.